AD 676318

DDC
OCT 22 1968

John S. Dunning
Douglas N. Bennion

THE ELECTROCHEMICAL REDUCTION OF META-DINITROBENZENE IN DIMETHYLSULFOXIDE

July 1968
Report No. 68-40

This document has been approved for public release and sale; its distribution is unlimited.

CLEARINGHOUSE

Report No. 68-40
July 1968

THE ELECTROCHEMICAL REDUCTION OF META-DINITROBENZENE IN DIMETHYLSULFOXIDE

John S. Dunning
Douglas N. Bennion, *Principal Investigator*

July 1968

Financial Support Provided through
Contract No. N123-(62738)57439A
U. S. Naval Weapons Center
Corona, California

DEPARTMENT OF ENGINEERING
UNIVERSITY OF CALIFORNIA
LOS ANGELES

FOREWORD

This report, in all essential respects, is the Master of Science thesis of John S. Dunning, as accepted June 1968. Thanks are due to the authors' co-workers, Dr. E. d'Orsay, Mr. Mike Yao, and Mr. Bill Tiedemann, whose suggestions and discussions were most helpful.

The authors are particularly grateful to the Electrochemistry Branch of the Naval Weapons Center, Corona, California, which provided financial support for this study through Contract No. N123-(62738)574939A.

ABSTRACT

The electrochemical reduction of meta-dinitrobenzene in solutions of dimethylsulfoxide was studied on platinum electrodes. The object of the investigation was to determine the number of electrons transferred and the mechanism of transfer in the presence and absence of a proton donor, ammonium perchlorate.

Two independent electrochemical methods are used. They are the rotating disk electrode technique and the potentiostatic step technique. Measurement of the diffusion coefficient of meta-dinitrobenzene in the electrolyte solutions is done for use in the electrochemical calculations. A separate study of the temperature dependence of the solubility of m-DNB in DMSO is also done.

The electrochemical reduction in the absence of a proton donor takes place in two steps, which correspond to the formation and reduction of the m-DNB radical anion. When a proton donor is added, a homogeneous reaction takes place in the solution near the electrode which results in an effective increase in the number of electrons to four, corresponding to the reduction to nitrophenylhdroxylamine.

In separate studies, the diffusion coefficient of m-DNB in DMSO is found by the diaphragm cell method to be 6.15×10^{-6} cm^2/sec. The solubility is found to increase from 3.51 molal at 24°C to 4.64 molal at 49.75°C.

TABLE OF CONTENTS

	Page
LIST OF FIGURES	ix
LIST OF TABLES	xi
LIST OF SYMBOLS	xiii
INTRODUCTION	1
1. Background	1
2. Statement of the Problem	4
3. Rotating Disk Electrode Technique	5
4. Potentiostatic Step Technique	6
5. Diaphragm Cell Method for Diffusion Coefficients	7
EXPERIMENTAL	9
1. Solubility	9
2. Diffusion Coefficient	10
3. Rotating Disk Electrode	12
4. Potentiostatic Step	18
RESULTS AND DISCUSSION	23
1. Solubility	23
2. Diffusion Coefficient	25
3. Rotating Disk Electrode	28
4. Potentiostatic Step	39
5. Interpretation	43
CONCLUSIONS	51
BIBLIOGRAPHY	53
APPENDICES	
APPENDIX I	55
APPENDIX II	59
APPENDIX III	61
APPENDIX IV	63
APPENDIX V	65

LIST OF FIGURES

Figure		Page
1	Diffusion Cell	11
2	Rotating Disk Apparatus	13
3	Rotating Disk Assembly	14
4	Rotating Disk Electrical Circuit	16
5	Potential Step Cell	19
6	Potential Step Electrical Circuit	20
7	Solubility of m-DNB in DMSO as a Function of Temperature	24
8	Differential Heat of Solution Plot for Solubility of m-DNB in DMSO	26
9	Current-Voltage Curve for Reduction of M-DNB in the Absence of Proton Donors on the Rotating Disk Electrode	29
10	Current-Voltage Curves as a Function of Rotation Speed for m-DNB in DMSO in the Absence of Proton Donors	30
11	Limiting Current Dependence on $\omega^{\frac{1}{2}}$ for 1st Wave in Absence of Proton Donors	32
12	Limiting Current Dependence on $\omega^{\frac{1}{2}}$ for 2nd Wave in Absence of Proton Donor	33
13	Dependence of $i_1/\omega^{\frac{1}{2}}$ on Concentration of m-DNB in the Absence of Proton Donors. First Wave	34
14	Dependence of $i_1/\omega^{\frac{1}{2}}$ on Concentration of m-DNB in the Absence of Proton Donors. Second Wave	35
15	Current-Voltage Curves for m-DNB Reduction as a Function of Proton Donor Concentration	37
16	The Effect of Addition of AP on the 1st Wave Reduction of m-DNB in DMSO	38
17	Current vs. Time$^{\frac{1}{2}}$ for 1st Wave Reduction of m-DNB in DMSO in the Absence of Protone Donors from Potential Step Method	40
18	Current vs. Time$^{\frac{1}{2}}$ for 2nd Wave Reduction of m-DNB in DMSO in the Absence of Protone Donors from Potential Step Method	41

LIST OF FIGURES (Continued)

Figure		Page
19	Concentration Dependence of the Quantity $i \cdot t^{\frac{1}{2}}$ for 1st and 2nd Waves in Reduction of m-DNB in DMSO in the Absence of Proton Donors by the Potential Step Method	42
20	Calculated Concentration Profile for m-DNB for the Potential Step Method	44
21	Distillation Column Apparatus	56
22	Calibration Curve for Determination of m-DNB Concentration by Spectrophotometric Means	60
23	Kinematic Viscosity of DMSO Solution as a Function of m-DNB Concentration	64
24	Ratio of Limiting Currents for 1st and 2nd Waves as a Function of Temperature in the Absence of Proton Donors	66
25	Diffusion Coefficient of m-DNB in DMSO Solutions as a Function of Temperature	67
26	Activation Energy Plot for Diffusion of m-DNB in DMSO Solutions	68

LIST OF TABLES

Table		Page
1.	The Effects of Proton Donor Addition on the Reduction of Hydrocarbons as Reported by Given and Peover	3
2.	Initial and Final Concentrations of the Diffusion Cell for Two Runs	27
3.	Measured Properties of Purified DMSO at 25 °C	57
4.	Calibration Readings for Spectrophotometric Determination of DMSO Concentration	59
5.	Karl Fischer Water Determination for Purified DMSO	62

LIST OF SYMBOLS

A	electrode area
AP	ammonium perchlorate
C	concentration
C^o	concentration in bulk of solution
D	integral diffusion coefficient
DMSO	dimethylsulfoxide
D_e	diameter of rotating disk electrode
e^-	electron
F	Faraday's constant
H	partial molar enthalpy
i	electrical current
i_l	diffusion limited current
j	molar flux
k	homogeneous reaction rate constant
KFR	Karl Fischer reagent
l	thickness of diaphragm
m_i	molality of species i
m-DNB	meta-dinitrobenzene
n	number of electrons transferred
p	pressure
q	effective cross sectional area of diaphragm
R	general form of hydrocarbon
R_g	gas constant
R_d	ratio of proton donor concentration to m-DNB concentration
Re	Reynolds number
r	distance (radial) from center of a spherical electrode
r_o	radius of spherical electrode
r	effective radius of a molecule
T	absolute temperature

LIST OF SYMBOLS (Continued)

t	time
u_e	fluid velocity at edge of rotating disk
V	volume
x	distance variable
β	cell constant of diaphragm cell
γ_i	activity coefficient (molal) of species i
δ	diffusion boundary layer thickness
δ_o	hydrodynamic boundary layer thickness
λ	reciprocal of reaction layer thickness
μ_i	chemical potential of species i
μ_i^o	chemical potential in standard state
ν	kinematic viscosity
η	viscosity
ϕ	generalized benzene ring
ΔH_{ds}	differential heat of solution

INTRODUCTION

1. Background. The subject of high energy density batteries using lithium as a negative electrode in a nonaqueous electrolyte system has been discussed by Jasinski.[1]

Among the promising nonaqueous electrolytes are those of the organic sulfur containing class.[2] Of these, one widely studied has been dimethylsulfoxide (DMSO). The solvent properties of DMSO have been reviewed by Smyrl.[3] An extensive review of electrochemistry in DMSO has been prepared by Butler.[4] DMSO has a fairly high dielectric constant of 46 to 47 at 25°C and has a liquid range between 18.5°C and 189°C at atmospheric pressure. It appears to be stable toward lithium and has exhibited a useful voltage range of about five volts before decomposition. Electrical conductances for some lithium salts in DMSO have been measured to be in the range of 7×10^{-3} $ohm^{-1}cm^{-1}$.[5] While this is a little low for battery applications, it is quite possible for some solutes that conductance will be over 10^{-2} $ohm^{-1}cm^{-1}$ at operating temperatures of 50°C.

Batteries using lithium as one electrode and using DMSO as the solvent appear to be feasible if a suitable positive (cathode on discharge) electrode reaction can be found. The reduction of m-DNB has been used for this purpose in high energy, short life batteries with liquid ammonia solutions used as electrolytes.[6] Based on an open circuit voltage of 2.5 volts, a lithium/m-DNB couple has a theoretical energy density of about 1380 watt-hours per pound if the m-DNB were reduced completely to the dianiline. The study of the reduction of m-DNB in DMSO solutions is thus a natural extension of the search for high energy battery systems. This study is concerned with the mechanism of the reduction.

A survey of the literature shows many studies of organic electrochemical reductions in both aqueous and nonaqueous media. The effects of proton donor addition have been investigated for a number of systems. A few of the important references are summarized here as an introduction to the general problem.

In the absence of proton donors, Hoijtink et al.[7] found that the chief steps in the redu tion of various alternant and nonalternant hydrocarbons could be described as follows:

$$R + e^- \rightarrow R^- \qquad \text{I}$$

$$R^- + e^- \rightarrow R^= \qquad \text{II}$$

The first reaction is the formation of a radical anion by a reversible one electron transfer. The second reaction is the reduction of the radical anion. Reaction II occurs at more negative potentials than reaction I giving rise to two wave behavior on a dropping mercury polarogram.

The product of reaction I may also diffuse into the bulk of the solution and react with a hydrogen ion to form RH which then may dimerize or disproportionate. $R^=$ will also diffuse into solution to react eventually with hydrogen ions to form RH_2.

If a proton donor is present in the solution, the nature of the reduction process becomes quite complicated and many types of behavior are displayed. Given and Peover,[8] upon investigation of the reduction of aromatic hydrocarbons and carbonyl compounds in dimethylformamide, found that five different types of behavior resulted from the addition of phenol and benzoic acid. Their results are summarized in Table 1. It is interesting to note the differences in behavior of the same reactant due to differences in proton donors. It appears that the proton donating ability of the benzoic acid is greater than that of the phenol and that one might expect class E behavior in strongly acidic solutions, other things being equal.

Kolthoff and Reddy[9] have reported that the reduction of benzoquinone and quinhydrone in .1M tetraethylammonium perchlorate (TEAP) solutions in DMSO gave two waves. The first corresponds to a one electron reversible step while the second wave corresponds to an irreversible addition of, effectively, less than one electron. Upon addition of proton donors like hydrochloric acid, the second wave shifted to more positive potentials. This corresponds to class D behavior reported in Table 1.

TABLE 1

THE EFFECTS OF PROTON DONOR ADDITION ON THE REDUCTION OF HYDROCARBONS AS REPORTED BY GIVEN AND PEOVER.[8]

	Behavior	Explanation
Class A	1st wave height increases as 2nd wave height decreases.	$R^- + H^+ \rightarrow RH\cdot$ RH· reduced at same potential as R.
Class B	New wave between 1st and 2nd wave appears and grows in height as 2nd wave decreases.	Dimerization of R'.
Class C	Both waves grow in height; new waves may appear.	a) $R^- + H^+ \rightarrow RH\cdot$ RH· reduced at same potential as R. b) Protonation makes further reduction possible; mechanism undetermined.
Class D	1st wave stays the same but 2nd wave shifts to less negative potentials.	$R^=$ protonated but R^- is not.
Class E	New wave at less negative potentials appears; grows as the original waves decrease.	Prior protonation of R to RH^+.

Kemula and Sioda[10] have reported the behavior of two nitrocompounds in dimethylformamide (DMF). They found that the addition of benzoic acid to nitrosobenzene with $NaNO_3$ as supporting electrolyte caused the appearance of a new wave at less negative potentials than the first wave. This is clearly class E behavior. The addition of benzoic acid to nitrobenzene caused an increase in the height of the first wave to the height of both waves observed in the absence of benzoic acid. This is an example of a nitrocompound displaying type A behavior. The conclusions of Kemula and Soida were that the reduction of the aromatic nitro-group was a four electron reaction in the presence of a proton donor and that the first step represented the one electron formation of the free radical anion.

In a later study, Kemula and Sioda[11] reported the visible spectrum of the nitrobenzene free radical anion. Geske and Maki[12] have used ESR spectroscopy to study the electrochemical generation of nitrobenzene free radicals.

Tice, Cadle, and Chambers[13] have studied the reduction of several aromatic nitrocompounds as a function of the proton donor in solutions of acetonitrile, DMSO, propylene carbonate, and DMF. They found that trichloroacetic acid, p-toluenesulfonic acid, N, N diethylanilinium perchlorate, o-phthalic acid, salicylic acid, and p-hydroxybenzoic acid caused a new wave to appear at potentials more positive than the wave for the formation of the radical anion. All of these proton donors thus seem to produce class E behavior. Benzoic acid produced a wave which was merged with the one electron wave. Phenol, hydroquinone, and water at low concentrations did not produce class E behavior. It was also found that the reduction of p-chloronitrobenzene in o-phthalic acid solutions of acetonitrile resulted in a four electron wave using four moles of acid per mole of p-chloronitrobenzene. The reaction product was found to be p-chlorophenylhydroxylamine so that the overall reaction was:

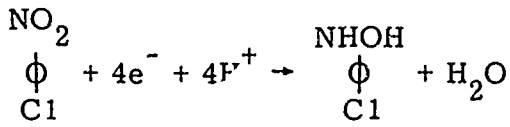

$$\underset{Cl}{\overset{NO_2}{\phi}} + 4e^- + 4H^+ \rightarrow \underset{Cl}{\overset{NHOH}{\phi}} + H_2O$$

It is interesting to note that the complete reduction to the aniline, involving six electrons and six hydrogen ions, was not observed. Apparently the phenylhydroxylamine is resistant to further reduction and only four electrons are transferred for each nitro-group.

2. Statement of the Problem. The purpose of this study was to determine the number of electrons transferred in the reduction, on a platinum electrode, of m-DNB in DMSO in the presence and absence of a proton donor, ammonium perchlorate. Two independent electrochemical methods were used for the determinations. These were the rotating disk electrode technique and the potentiostatic step technique. Information regarding the details of the reduction was to be derived from the electrochemical measurements.

In order to use the electrochemical techniques proposed, determinations of the diffusion coefficient and kinematic viscosity of m-DNB in DMSO were necessary. The diffusion coefficient was measured by means of the diaphragm cell method and the kinematic viscosity was measured with an Ubbelohde viscometer. In addition, a separate study of the solubility of m-DNB in DMSO was to be done as a function of temperature.

3. Rotating Disk Electrode Technique. The basis of the rotating disk technique is the solution of the Navier-Stokes equations for a disk rotating about an axis perpendicular to its face in a stationary, infinite, incompressible fluid. The resulting velocity profile for the system is then used in the convective diffusion equation. Using Fick's first law and the boundary condition that at the surface of the disk the concentration of the species in question is zero, the solution to the convective diffusion equation yields the limiting diffusional flux of the species toward the disk. Levich[14] has developed the equations describing this phenomenon. Riddiford[15] has published a comprehensive review of the technique.

Electrochemical reactions can be investigated if the rotating disk surface is an electrode. Observation of current through the electrode versus the potential difference between the electrode and the solution will show the point at which the flux to the surface becomes diffusion limited. At this point a small increase in the current will cause a large change in potential difference as a new reaction must begin to account for the increased current. Levich gives the following expression for the limiting current:

$$i_{lim} = 0.62\, nFD^{2/3} \nu^{-1/6} \omega^{1/2} C^{o} A \qquad (1)$$

where

- n = number of electrons transferred in the electrode reaction per mole of the active species.
- F = Faraday's constant.
- D = integral diffusion coefficient of the active species.
- ν = kinematic viscosity of the bulk solution.
- C^{o} = concentration of the active species in the bulk solution.
- ω = angular rotational velocity of the electrode.
- A = area of the electrode.

Newman[16] has shown that for large Schmidt numbers the value of the numerical constant in Equation (1) can be corrected to give:

$$i_{lim} = \frac{0.554\ nFD^{2/3}\nu^{-1/6}\omega^{1/2}C^{o}A}{.8934\left(1+.298\ Sc^{-1/3}+.14514\ Sc^{-2/3}\right)} \tag{2}$$

If a limiting diffusional current can be obtained experimentally, Equation (1) and Equation (2) can be used to determine the number of electrons transferred if the other parameters are known. The kinematic viscosity and diffusion coefficients can be measured by standard methods. The bulk concentration and rotation speeds can be controlled for the experimental measurements. The electrode area can be measured accurately. Thus the rotating disk electrode gives a steady state method of determining the number of electrons transferred at an electrode surface.

4. Potentiostatic Step Technique. The potentiostatic step technique, as applied to a spherical electrode, involves the solution of the semi-infinite spherical diffusion equation. This technique has been described by Delahay.[17] A sudden change in the potential difference between the electrode and the surrounding solution is applied. The magnitude of the change is such that the species of interest is electrolyzed at a very high rate. The boundary condition of zero concentration of active species at the electrode surface is thereby established. The concentration distribution resulting from the imposition of the step is a function of time as follows:

$$C(r,t) = C^{o}\left[1 - \frac{r_o}{r}\ \mathrm{erfc}\left(\frac{r-r_o}{2D^{\frac{1}{2}}t^{\frac{1}{2}}}\right)\right] \tag{3}$$

where the complementary error function is defined by

$$\mathrm{erfc}\,\lambda = 1 - \frac{2}{\pi^{\frac{1}{2}}}\int_0^{\lambda} \exp\left(-Z^2\right) dZ \tag{4}$$

and

D = integral diffusion coefficient of the active species.
r = distance from the center of the electrode.
r_o = radius of the electrode.
t = time from application of the potential step.

The current at the surface of the electrode is obtained by evaluating the concentration gradient at the surface:

$$D \left.\frac{dC}{dr}\right|_{r=r_o} = \text{flux at the surface} \tag{5}$$

which gives, for the current

$$i = nFA\,D^{\frac{1}{2}}C^{o}\,\frac{1}{\pi^{\frac{1}{2}}t^{\frac{1}{2}}} + nFA\,D\,C^{o}\,\frac{1}{r_o} \tag{6}$$

where n, F and A have the same meanings as for the rotating disk electrode.

In general, for short times (less than 2 seconds) and large r_o (greater than .50 mm.), the second term in Equation (6) can be neglected compared to the first term. If the time of reaction is too long, natural convection is set up by the differences in density between product and reactant solutions near the electrode. In this case Equation (6) is not valid.

If experimental results indicate that Equation (6) is being obeyed, then the number of electrons transferred can be calculated if the diffusion coefficient is known. The bulk concentration is used as the experimental variable, along with the time of electrolysis.

5. Diaphragm Cell Method for Diffusion Coefficients. The diaphragm cell method of determining diffusion coefficients has been discussed by Stokes.[18] It is an unsteady state method in which a concentration gradient is set up in the pores of a sintered glass disk. In this manner mechanical and thermal disturbances in the surroundings have no effect on the diffusion because convection within the diaphragm is prevented. In addition, large concentration gradients can be used, so that short runs can be made. Because of these advantages over other methods, as well as the simplicity of the experiment, the diaphragm cell method was chosen to determine the integral diffusion coefficient to be used in the electrochemical experiments.

The cell is characterized by a vertical tube in which solutions in the top and bottom compartments are separated by a horizontal sintered glass disk. The pores of the disk must be small enough to prevent streaming and convection between the solutions and large enough to eliminate wall effects of the pores.

Different experimenters have found a pore diameter of 10^{-3} to 10^{-4} cm. to be satisfactory. Within each compartment of the cell complete mixing is accomplished by means of mechanical stirrers.

The equations describing the mass transfer for a system such as the one above can be written.

$$V_t dC_t + D q/l (C_t - C_b) dt = 0 \tag{7}$$

$$V_b dC_b + D q/l (C_b - C_t) dt = 0 \tag{8}$$

In these equations C_t and V_t refer to the concentration and volume of the top compartment and C_b and V_b refer to the lower compartment. The effective cross-section of the disk is denoted by q, and l refers to the thickness of the diaphragm. If Equations (7) and (8) are combined and D is assumed independent of concentration, we get:

$$\frac{d(C_t - C_b)}{(C_t - C_b)} + \beta D dt = 0 \tag{9}$$

where β is the cell factor, given by

$$\beta = q/l \left(\frac{1}{V_t} + \frac{1}{V_b}\right) \tag{10}$$

Integrating Equation (9), the result is

$$\ln \frac{(C_t - C_b)_{initial}}{(C_t - C_b)_{final}} = - \beta D t \tag{11}$$

Thus if the initial and final concentrations in each compartment, the cell factor, and the time of the experiment are known, the integral diffusion coefficient can be calculated.

The measurement of the cell factor is usually done by calibrating the cell with a solution whose diffusion coefficient is well known. Gordon[19] recommends that KCℓ be used as a calibrating solution at .1 N and 25°C. He suggests the value of $D = 1.838 \times 10^{-5}$ cm^2/sec for small concentration differences between compartment concentrations. Stokes[20] gives a very complete set of calibration data.

EXPERIMENTAL

1. Solubility. The solubility of m-DNB in DMSO was determined as a function of temperature at atmospheric pressure. Measurements were carried out in a dry atmosphere glove box using purified DMSO. The purification procedure is described in Appendix I. The temperature of the solution was controlled by placing it in a double walled vessel with water used as the heating and cooling medium. The water temperature was controlled by a mercury contact temperature bath to ±0.01°C. Temperatures of the solution were measured by a copper-constantan thermocouple as well as with a calibrated thermometer. Stirring of the solution was accomplished by means of a magnetic stirring bar.

The temperature of the solution was raised to approximately 50°C to start the experiment. A period of one week was allowed initially for the solution to reach equilibrium before samples were taken. The temperature was lowered after each sample was taken and the system was allowed to equilibrate for at least 24 hours. About half of the samples were taken in this manner. Then the temperature was raised after each sampling and the system again was allowed 24 hours to come to equilibrium. There was no systematic variation of the measured solubilities between the two methods of changing temperature.

Samples were withdrawn using a 10ml. pipet. The pipet was heated to the temperature of the bath to minimize crystallization in the pipet. The pipet volume change due to thermal expansion was negligible. A glass wool filter was used to keep undissolved particles of m-DNB out of the pipet. The pipet was washed with 10 ml. of pure DMSO after transferring the original contents to a 100 ml. volumetric flask. This wash was also put into the volumetric flask. After several samples had been taken, the volumetric flasks were removed from the dry box and each was filled to the 100 ml. mark.

The samples were then diluted again to either 1/20 or 1/40 of the saturated concentrations in order to put the concentration in a range convenient for analysis. The concentration was determined using a Beckman model DU spectrophotometer. A light wavelength of 420 millimicrons and a slit width of 0.22 mm. were found to give good calibration readings. It was found that for

m-DNB in DMSO Beer's law is followed up to concentrations of about 30 mg. of m-DNB per ml. of solution. Instead of taking readings in this range, it was decided to calibrate the absorbance versus concentration curve up to 90 mg. /ml. and fit the data with a quadratic equation. See Appendix II for a detailed account of the method used. This procedure reduced dilution errors and gave less scatter of the actual solubility data than would have been obtained if concentrations were determined in the linear absorbance-concentration region.

2. Diffusion Coefficient. It was necessary to measure the diffusion coefficient of m-DNB in the supporting electrolyte solution used in the electrochemical experiments. The diaphragm cell method of Stokes[18] was chosen for use in these measurements.

The glass cell is shown in Figure 1. It consisted of two compartments separated by a porous glass diaphragm 10 mm. in diameter and 3 mm. thick. It had a pore size of 10-15 microns. Stirring was accomplished by magnetically driven glass stirring bars located on each side of the diaphragm. A large U-shaped magnet, mounted externally to the cell, and rotated by a variable speed motor, provided the driving force. The cell was operated in a vertical position with the upper compartment containing the dilute solution and the lower compartment the more concentrated solution. The stirring bars were so constructed that the one in the lower compartment floated to the top and rested on the diaphragm while the one in the upper compartment sank to the bottom and rested on the diaphragm. This arrangement enabled the bars to sweep the surface of the diaphragm and provided for reproducible stirring. The stirring rate was 60 RPM.

The cell was similar to that of Stokes,[18] but was modified to provide for only glass and teflon to be in contact with the solution. This was to prevent DMSO from dissolving the grease and rubber present in Stokes' cell. Telflon stopcocks were used for filling and draining the cell and teflon sleeves were used on all ground glass joints.

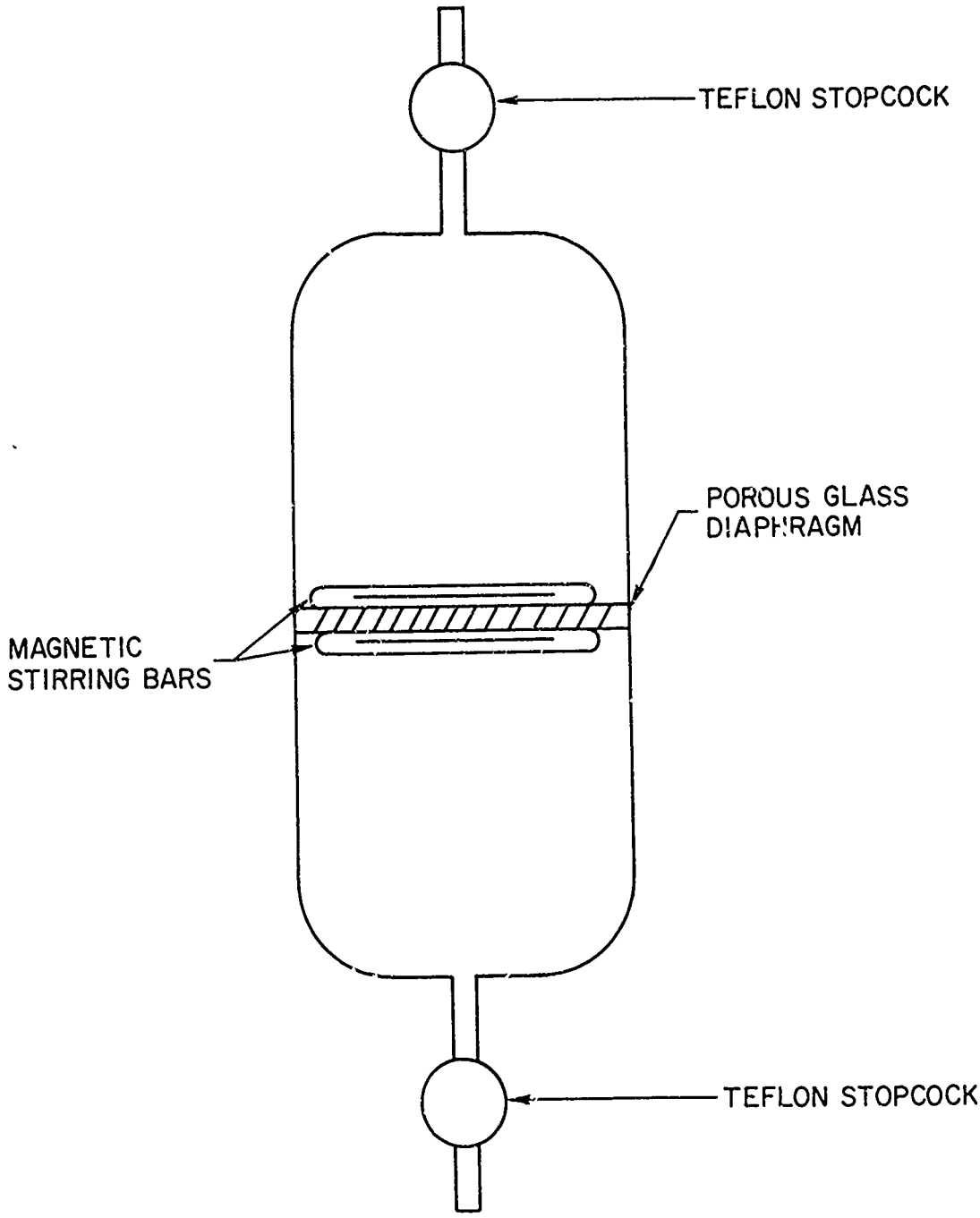

DIFFUSION CELL

Figure 1

The experimental procedure described by Stokes was followed. All measurements were taken in a water bath held at 25.0 ± .1 ^{o}C. Calibration of the cell was done with the lower compartment filled with a 0.1 N potassium chloride-water solution and the upper compartment filled with redistilled water. Analysis of the final solutions was done by precipitating the chloride ion as AgCℓ and weighing. The durations of the calibration runs varied from 175 minutes to 7180 minutes. The average cell constant was β = 6.19 cm^{-2} with an average deviation of 9.2%.

Two runs were made to determine the diffusion coefficient of m-DNB in 0.1M tetraethyl ammonium perchlorate (TEAP) solutions in DMSO. The first lasted 5840 minutes and measured D in the range between 0.0381 M m-DNB and pure supporting electrolyte. The second run was for 8225 minutes and the D measured was for concentrations between 0.05 M m-DNB and the pure supporting electrolyte. These concentrations represent the initial conditions.

The concentrations of m-DNB (initial and final) in the two compartments were determined by spectrophotometric means described in Appendix II.

3. Rotating Disk Electrode. The rotating disk electrode equipment is shown in Figure 2. It consisted of a variable speed motor which drove a rotating shaft by means of pulleys. The motor was isolated by rubber vibration damping mounts and the electrode drive shaft ran through a Dumore quill bearing system. The electrode was very carefully mounted so that vibration was kept at a minimum.

The electrode assembly is shown in Figure 3. The working electrode surface was a cross-section of platinum wire of 0.258 cm. diameter. The wire was force-fitted through a teflon shaft of 3 cm. diameter. The teflon was in turn force-fitted to a steel shaft which was placed in the chuck of the quill. Copper wire made the electrical connection between the steel and platinum. The pick-up on the rotating shaft consisted of a silver slip ring and a spring loaded graphite rod which made the connection to the non-rotating electrical

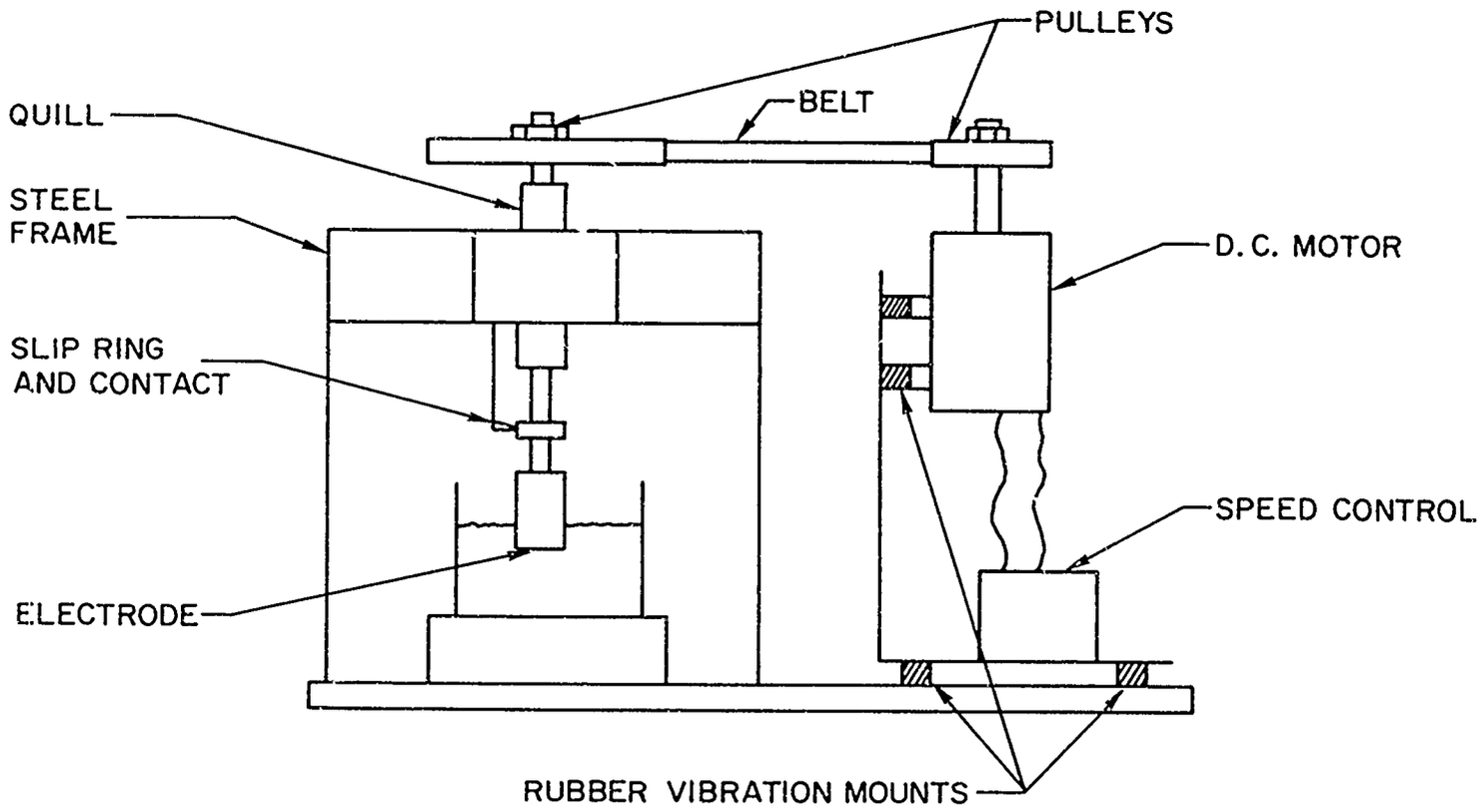

ROTATING DISK APPARATUS

Figure 2

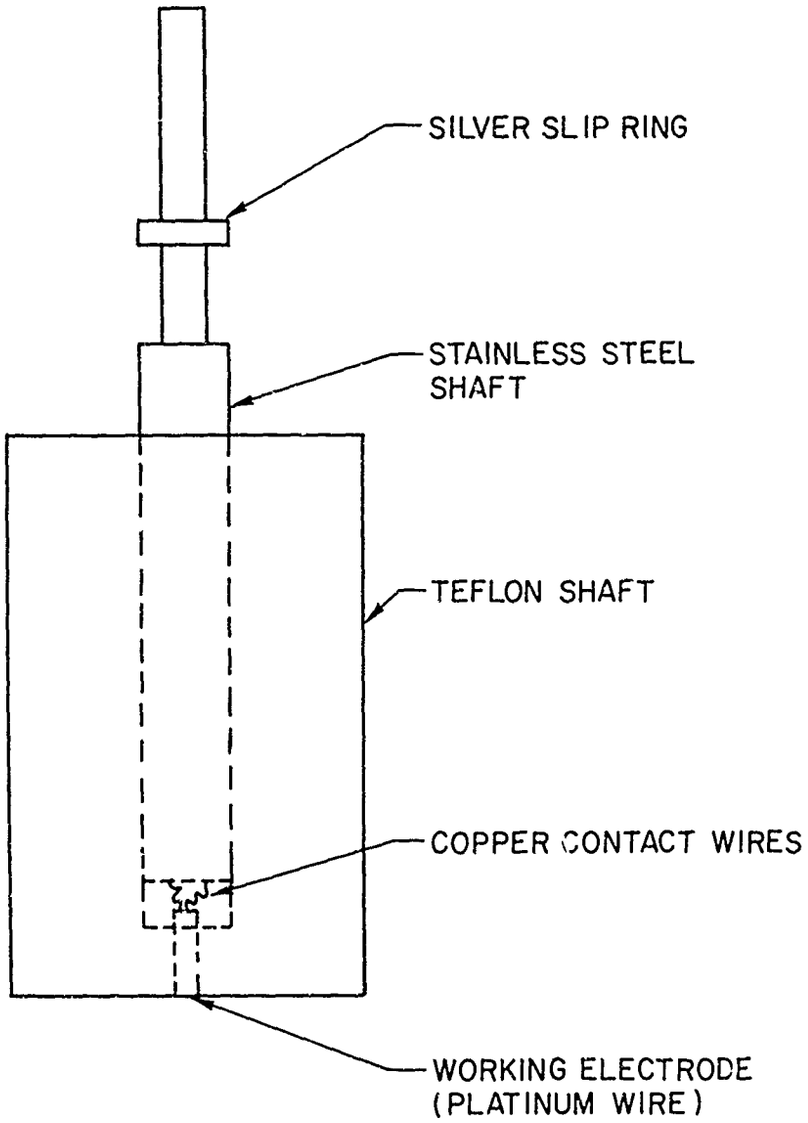

ROTATING DISK ELECTRODE ASSEMBLY

Figure 3

measuring system. The electrode was carefully machined to eliminate wobble and the face was polished to a mirror surface on #00 emery paper.

The speed of rotation of the disk was made variable by two means. First, the drive motor was a universal motor controlled by a variac speed control with speeds from 0 to 8800 RPM. Secondly, speed variation could be accomplished by changing the pulley combination on the motor and the drive shaft. The speed was monitored by a General Radio strobotac accurate to ±.5%.

The circuit used for the galvanostatic polarization of the rotating disk electrode is shown in Figure 4. The power supply used was a Heathkit model IP-32 Regulated Power Supply having a range of 0 to 400 volts and a maximum current output of 100 milliamps. The voltmeter was a Keithley model 610B electrometer with rated input impedance in excess of 10^{12} ohms. The ammeter was a Simpson model 262 volt-ohm-milliammeter with a sensitivity of 1.0 microamp on the finest scale. The variable resistor was a Clarostat Power Resistor decade box, which was set at 999,999 ohms.

The voltages measured were compared to either a saturated $Ag/AgC\ell O_4$ reference electrode or to the platinum counter electrode. The counter electrode had an area of 10 cm^2. Since this is 3000 times the area of the working electrode, the counter electrode was considered nonpolarizable and therefore suitable for a reference electrode.

The $Ag/AgC\ell O_4$ reference electrode consisted of a tube of pyrex glass with one end sealed with soft glass. The soft glass cracked on cooling, allowing good ionic conduction but negligible diffusion through the cracks. A saturated $AgC\ell O_4$ solution in DMSO was placed in the tube and a coil of shiny silver wire put in contact with the solution and $AgC\ell O_4$ crystals in the tube. The open end of the tube was sealed to prevent atmospheric contamination of the solution. The cracked glass tip was placed as near as possible to the working electrode when measurements were being taken.

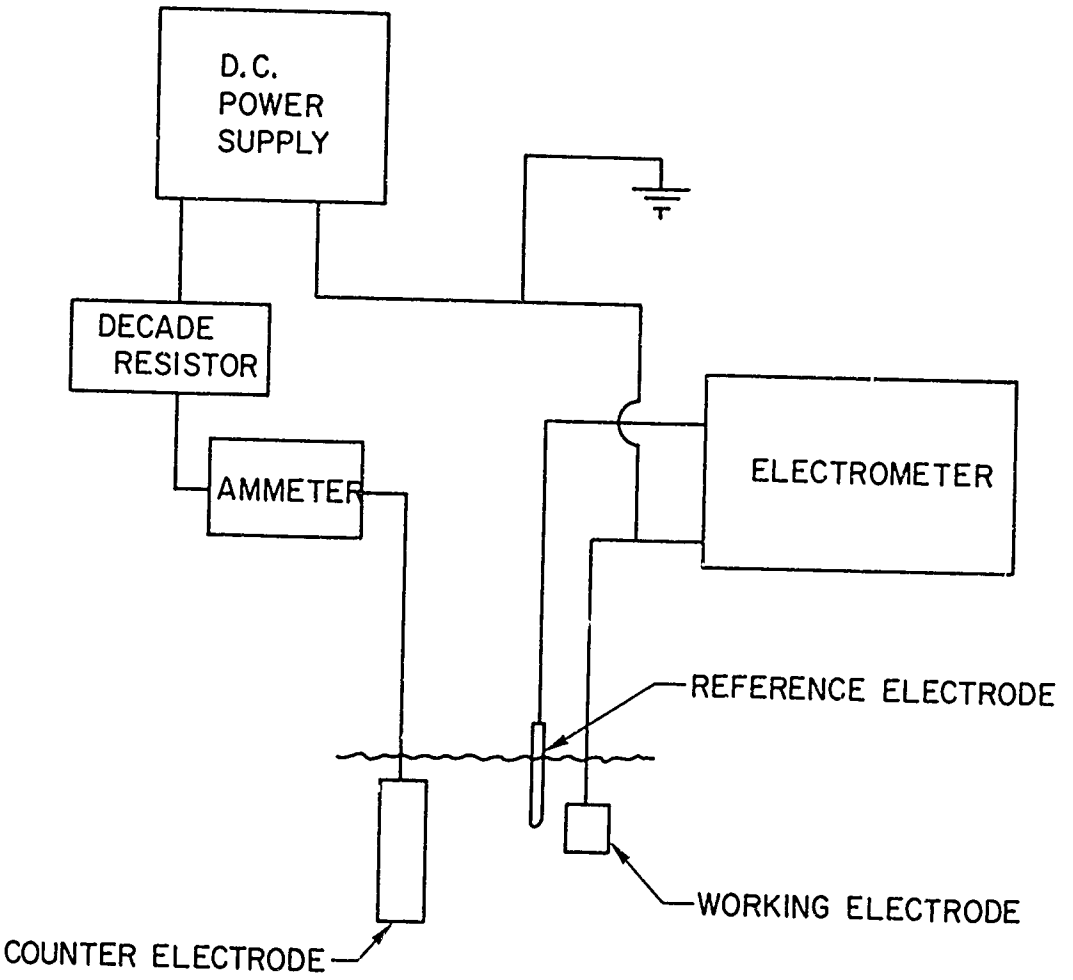

ELECTRICAL CIRCUIT - - ROTATING DISK ELECTRODE

Figure 4

The reaction vessel contained approximately 250 ml. of solution. The counter electrode was placed directly in the solution, at a distance of 3 to 4 cm. from the working electrode.

The platinum working electrode was cleaned with a saturated solution of ferrous sulfate in sulfuric acid. It was washed with distilled water and rinsed with the test solution before each run. Between experimental runs, the electrode was carefully re-polished with soft tissue. The cell was washed and dried whenever a fresh solution was being used.

The potential-current curves were generated by adjusting the power supply so that a constant, known current was passed between the counter electrode and the working electrode. The resulting steady state potential difference between the working electrode and the reference electrode was noted. Steady state may be defined for the purpose of this report as the condition when the potential is constant within 10 millivolts for ten minutes. At currents greater than 10 microamps, steady state potential differences were attained within two minutes of the application of the current. Below 10 microamps, somewhat longer times, on the order of 10 minutes, were necessary for steady state to be reached.

Current-potential curves were generated for a number of rotation speeds for each concentration investigated. The speeds ranged from 200 RPM to 1200 RPM. The concentrations of m-DNB ranged from 0.01 M to 0.04 M.

The effects of water content on the results of the rotating disk experiments were examined. Distilled DMSO with water content below 100 ppm was used in a sealed cell under a dry nitrogen atmosphere. The m-DNB was recrystallized three times from methanol and the melting point was determined to be 89 ^{o}C, which is in good agreement with the literature values. The tetraethylammonium perchlorate and ammonium perchlorate used were dried in a vacuum oven for 24 hours at 80-100 ^{o}C.

It was found that increasing the water content of the DMSO up to 0.2% did not change the results of the experiments. This is illustrated by Figures 13 and 14 in which the m-DNB concentration of .02 represents the data found

with the purified system and the other points represent the results obtained with the reaction vessel open to the atmosphere. These tests were done at ambient (22-24°C) temperatures.

In addition to the above study, the effect of adding NH_4^+ ion, as dissolved ammonium perchlorate, was investigated. For these measurements, a 0.02M m-DNB solution was used at a rotation speed of 300 RPM. Limiting currents were recorded as a function of the concentration of the ammonium ion.

4. Potentiostatic Step. The cell used for the potentiostatic step experiments is shown in Figure 5. The working electrode was a platinum ball with an area of $8.55 \times 10^{-2} cm^2$. The ball was formed by melting the tip of a piece of platinum wire in an oxygen-gas flame. The wire was then sealed into a thin pyrex glass tube attached to a ground glass joint for fitting through the top of the cell. The apparent area of the ball was determined by optical magnification of the electrode and subsequent measurement. The counter electrode was a large cylinder of platinum wire screen which surrounded the working electrode at a distance of about 1.5 cn. Various ports were provided in the cell for purging and reference electrode placement. Approximately 190 ml. of solution were contained in the cell. The cleaning procedure for the cell was essentially the same as that described for the rotating disk electrode.

The circuit used to set the potential for the step and to measure the current decay is shown in Figure 6. The potential was set with an Anotrol Model 4100 Research Potential Controller. Current was measured as a function of the time from the application of the potential step. This was done with a Tektronix 545-A oscilloscope fitted with a Polaroid camera. The oscilloscope measured the potential drop across a General Radio precision decade resistor with an accuracy of 0.01 ohms. A photograph of the decay of this potential drop as a function of the time from the application of the potential step was obtained. From this the current-time curve was calculated. The times involved in the experiment were from 0.2 sec to 2.0 seconds from the application of the potential step. The rise time of the potentiostat is on the order of one millisecond or less.

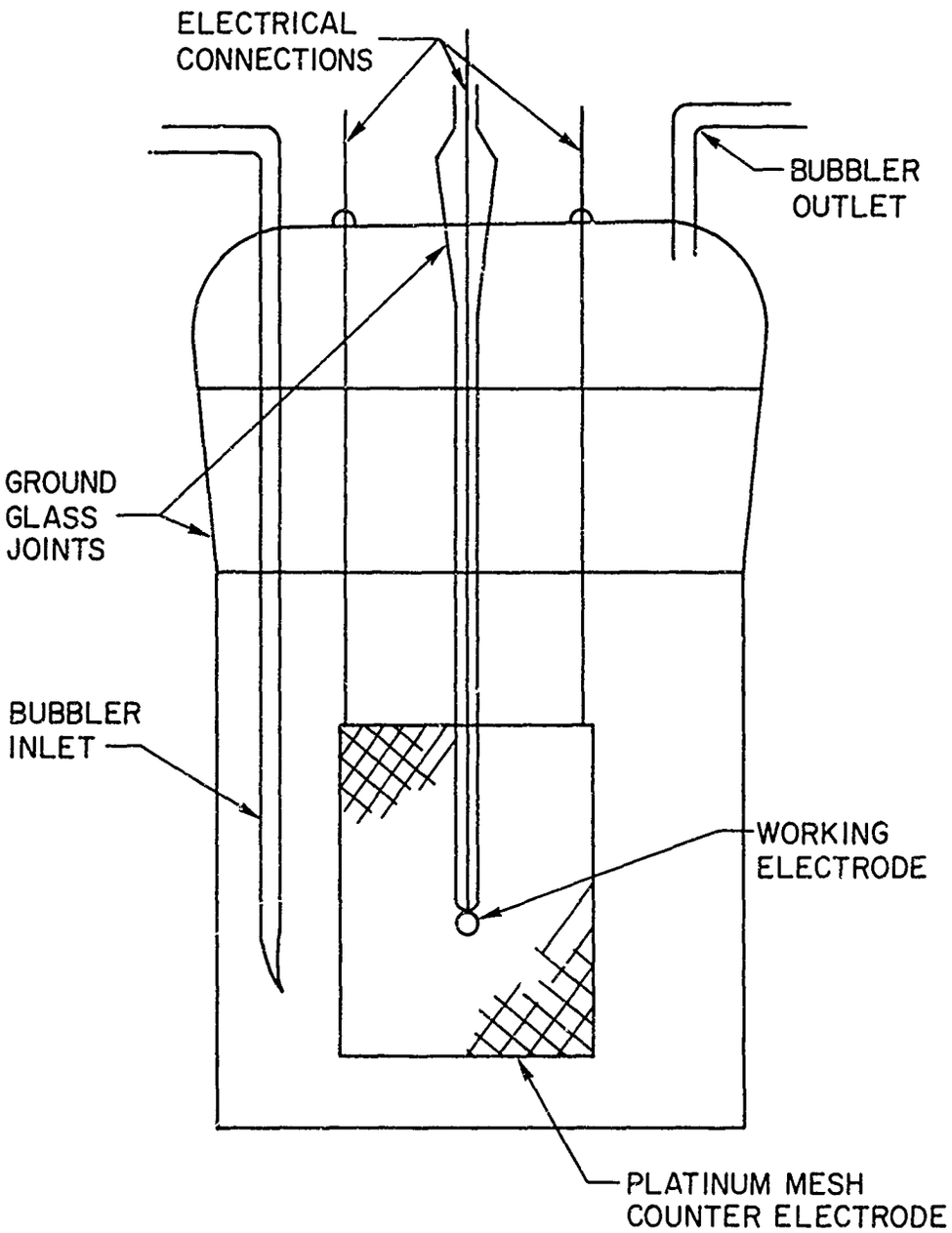

POTENTIAL STEP CELL

Figure 5

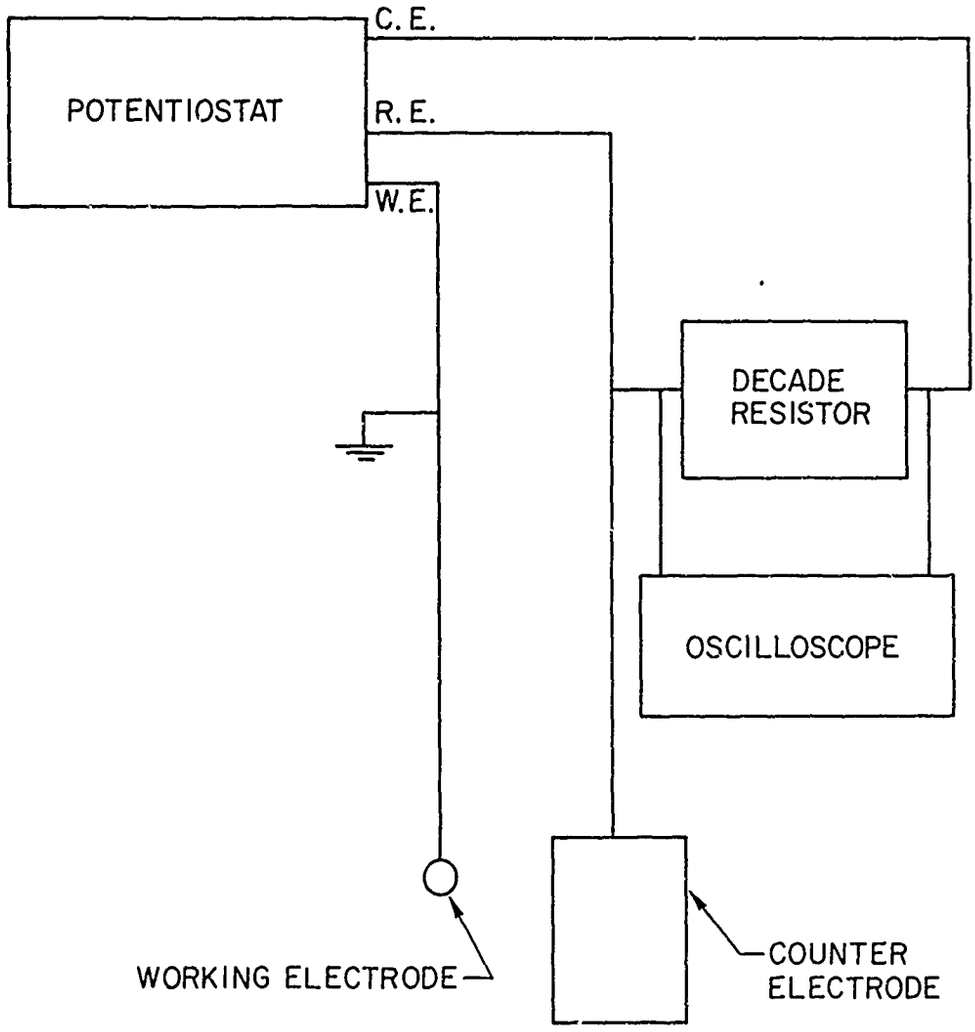

POTENTIAL STEP CIRCUIT

Figure 6

The value of the potential imposed by the potentiostat must be sufficient to produce zero concentration of m-DNB at the surface of the electrode, if Equation (6) is to apply. In order to get some idea of the potential necessary, a continuous voltage sweep polarogram was run on the solutions. The potential at which limiting currents were observed was used as the preliminary value to be imposed between the working and counter electrodes of the cell. For the first wave this potential was -1.8 V. For the second wave it was -2.3 V. This represents the potential of the working electrode relative to the counter electrode. It was found that when these potentials were applied during the experiments, the current-time curves corresponding to diffusion limitation of mass transfer were observed.

The first wave was investigated with five concentrations of m-DNB ranging from 8×10^{-3} to 4×10^{-2} M. The second wave was investigated with three concentrations in the same range. The supporting electrolyte, as in the rotating disk experiments, was 0.1 M tetraethylammonium perchlorate.

The potential step method was not applied to solutions containing ammonium perchlorate as a proton donor for two reasons. First, the addition of a proton donor changes the potentials at which the limiting currents occur. Thus the potential which must be set to produce this current was experimentally difficult to determine. This limitation does not apply to the rotating disk electrode system because the potential is the dependent rather than the independent experimental variable. The second reason that the potential step was not used for proton donor experiments is that it is an unsteady state method in which the diffusion layer thickness is changing with time. Thus, if the reaction is a complicated series of homogeneous and heterogeneous steps, the potential step method generates a series of time dependent species conservation equations which are difficult to solve. The rotating disk technique, on the other hand, is a steady state method which offers much simpler mathematical solutions when complicated mechanisms are involved.

RESULTS AND DISCUSSION

1. Solubility. It was found that the solubility of m-DNB in DMSO increased from 3.51 molal at 24°C to 4.64 molal at 49.75°C. The data is shown in Figure 7.

At saturation, the chemical potentials of the m-DNB (denoted by subscript i) are equal in the liquid and solid phases.

$$\mu_i^s = \mu_i^l \tag{12}$$

where

$$\mu_i = \mu_i^o + RT \ln \gamma_i m_i \tag{13}$$

and the convention is that

$$\gamma_i \rightarrow 1 \qquad \text{as} \qquad m_i \rightarrow m_{i,s} \tag{14}$$

where $m_{i,s}$ is the molality of m-DNB at saturation at the temperature and pressure of interest. At saturation, Equations (12) and (13) can be combined to give

$$\mu_i^s = \mu_i^o + RT \ln \gamma_i + RT \ln m_{is} \tag{15}$$

upon rearrangement,

$$\frac{\mu_i^s}{T} - \frac{\mu_i^o}{T} = R \ln \gamma_i + R \ln m_{is} \tag{16}$$

If Equation (16) is differentiated with respect to temperature, the result is

$$\left(\frac{\partial \mu_i^s/T}{\partial T}\right)_{p,SAT} - \left(\frac{\partial \mu_i^o/T}{\partial T}\right)_{p,SAT} = R\left(\frac{\partial \ln \gamma_i}{\partial T}\right)_{p,SAT} + R\left(\frac{\partial \ln m_i}{\partial T}\right)_{p,SAT} \tag{17}$$

But

$$\frac{\partial \mu_i^s/T}{\partial T} = -\frac{\overline{H}_i^s}{T^2} \tag{18}$$

PRECEDING PAGE BLANK

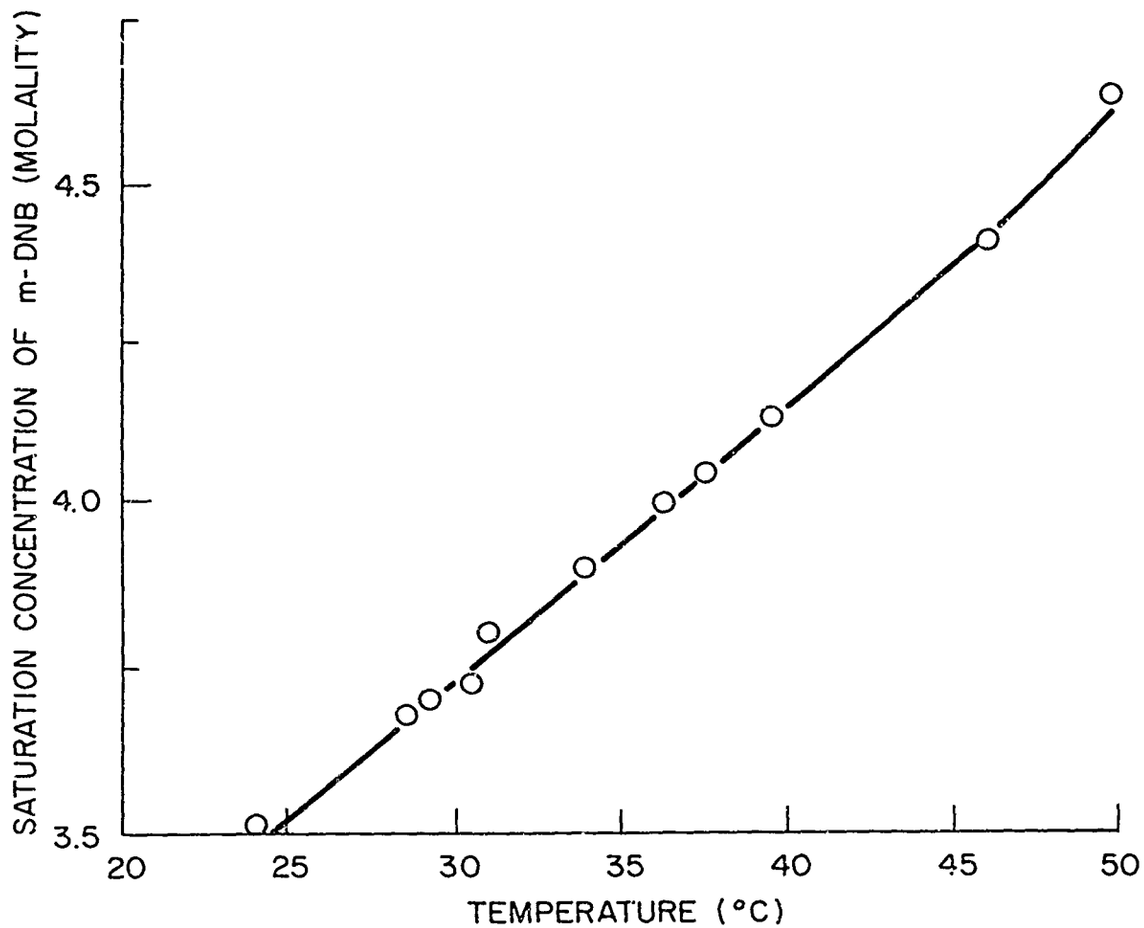

SOLUBILITY OF m–DNB IN DMSO AS A FUNCTION OF TEMPERATURE

Figure 7

and

$$\frac{\partial \mu_i^o/T}{\partial T} = -\frac{\overline{H}_i^o}{T^2} \tag{19}$$

where $\overline{H}_i^s$ is the partial molar enthalpy in the solid and $\overline{H}_i^o$ is the partial molar enthalpy in the saturated solution. Thus Equations (1∂), (18), and (19) combine to give

$$-\frac{\overline{H}_i^s}{T^2} + \frac{\overline{H}_i^o}{T^2} = R\left(\frac{\partial \ln \gamma_i}{\partial T}\right)_{p,\,SAT} + R\left(\frac{\partial \ln m_i}{\partial T}\right)_{p,\,SAT} \tag{20}$$

But by the convention adopted in Equation (14),

$$\left(\frac{\partial \ln \gamma_i}{\partial T}\right)_{p,\,SAT} = 0 \tag{21}$$

The resulting equation is:

$$\frac{\partial \ln m_{i,s}}{\partial 1/T} = \frac{\overline{H}_i^o - \overline{H}_i^s}{R} = \frac{-\Delta H_{DS}}{R} \tag{22}$$

where ΔH_{DS} is the differential heat of solution.

Figure 8 shows a plot of the experimental values of the logarithm of the molality versus the inverse of the temperature. From the slope of the plot the differential heat of solution was found to be 2053 cal/mole. The solid line in Figure 7 is a plot of the empirical equation for molality $m = 112.8 \exp(-2053/RT)$. This equation fits the data quite well in the temperature range considered.

2. Diffusion Coefficient. Stokes (18) has reported that accuracies of better than 1% can be obtained with the diaphragm cell technique. In this study deviations of up to 10% were found among the various calibration runs and in the final determination of the unknown diffusion coefficient. It is believed that the main cause of this error was the blockage of some of the pores in the diaphragm by air bubbles. Although the solutions were deaerated by evacuation with an aspirator water pump, some bubble formation was noted as the solution was sucked through the diaphragm to start the experiment. The

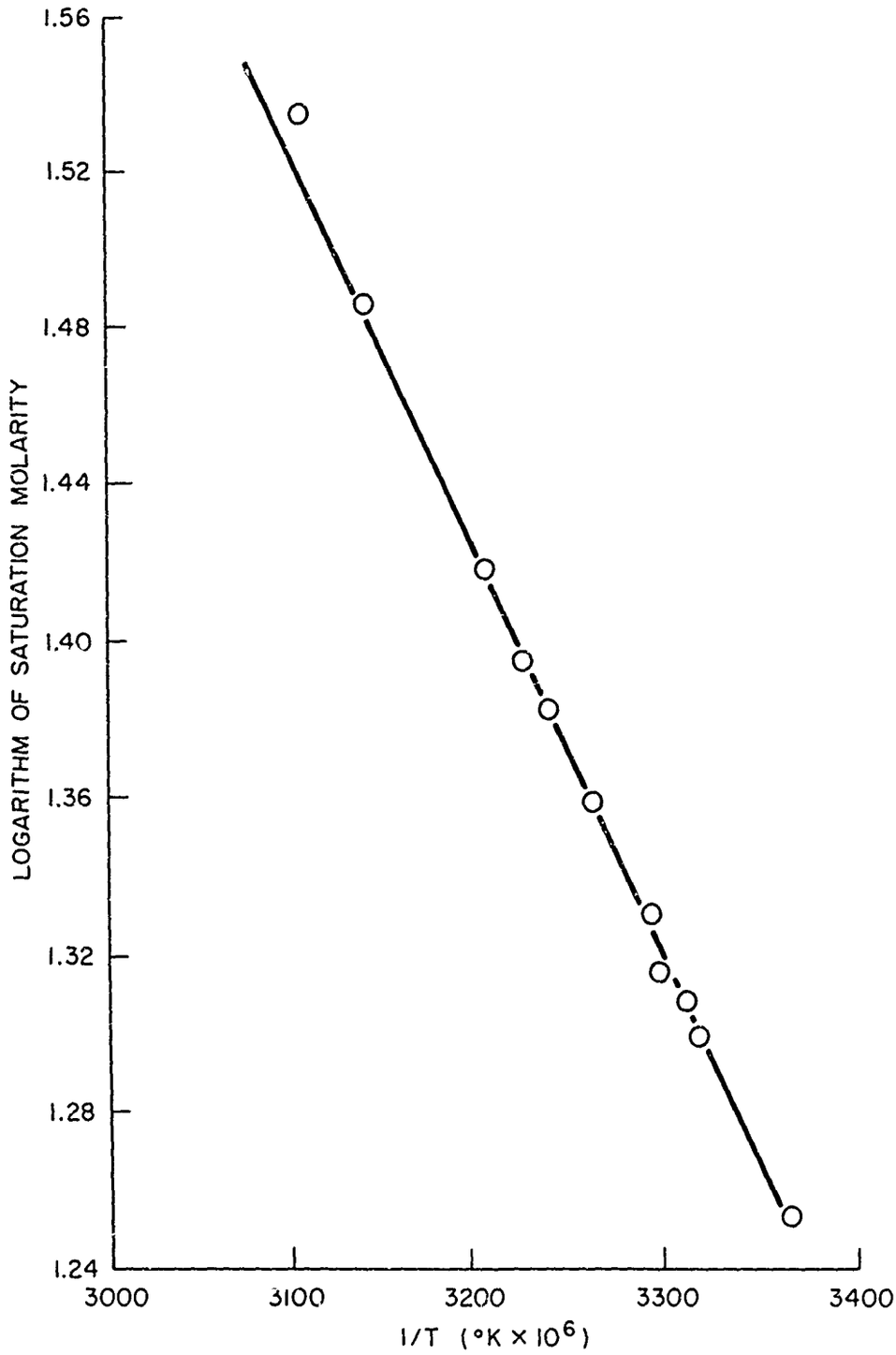

DIFFERENTIAL HEAT OF SOLUTION PLOT FOR SOLUBILITY OF m–DNB

Figure 8

compartments were refilled before the runs were started, but there is a possibility that some air was still trapped in the diaphragm. This would cause the cell "constant" to be different for different experimental runs, possible enough to account for the observed discrepancies.

The results of the two experiments to determine the diffusion coefficient of m-DNB in the solution of 0.1 M TEAP-DMSO are summarized in Table 2.

TABLE 2

INITIAL AND FINAL CONCENTRATIONS IN TOP AND BOTTOM COMPARTMENTS OF THE DIFFUSION CELL FOR TWO RUNS

Run no.	Time (min)	C^i top (molar)	C^f top (molar)	C^i bot (molar)	C^f bot (molar)
1	5840	0	.0042	.0381	.0363
2	8225	0	.0075	.0500	.0430

A simple analysis of the above data indicates some discrepancies. The volumes of the two compartments were determined by filling with water and weighing. They were 25.6 cm.^{3} for the bottom compartment and 25.7 cm.^{3} for the top compartment. Using these volumes, it is possible to calculate any one of the four concentrations in Table 2 from the other three. This can be done by means of the following molar balance:

$$C_t^f V_t - C_t^i V_t = C_b^i V_b - C_b^f V_b \tag{23}$$

The results of the first experimental run do not satisfy Equation (23). Because of this discrepancy the second run was undertaken. Run #2 gave much better agreement with Equation (23) and yielded a diffusion coefficient of 6.49×10^{-6} cm^2/sec. The value of C_t^f seems to be in error in run #1. This value was discounted and a "corrected" final dilute concentration of .0018M was calculated from Equation (23). The resulting diffusion coefficient was 5.81×10^{-6} cm^2/sec. The mean value of the two rums, used to analyze the electrochemical experiments, was $D = 6.15 \times 10^{-6}$ cm^2/sec $\pm 10\%$ This leads

to a discrepancy of ±4% in the value of $D^{\frac{2}{3}}$ used in the rotating disk experiments for determining the number of electrons.

The Stokes-Einstein relation for the effective radius of a large molecule diffusing through a continuum of smaller molecules is:

$$r = \frac{\kappa T}{6 \pi \eta D} \tag{24}$$

Using the value of the diffusion coefficient found and the other known parameters of Equation (24), r was calculated to be 1.82×10^{-8} cm. This radius is near the smallest dimension given by Kitaigorodskii[22] for the m-DNB molecule from crystallographic studies. The small value for the effective radius indicates that few, if any, solvent molecules are strongly associated with the m-DNB molecules in the solvation process in DMSO.

3. Rotating Disk Electrode. As the current through the cell containing the solutions of m-DNB in DMSO was increased by increasing the voltage output of the power supply, a red substance appeared on the surface of the electrode. This substance appeared to be quite soluble in DMSO. It was also less dense than the solution and floated to the top of the cell if the electrode was motionless. If no m-DNB was present in the cell, the red substance did not appear.

Figure 9 shows the dependence of the voltage on current for the galvanostatic reduction of m-DNB in a .1 M TEAP-DMSO solution. The voltage was measured versus the $Ag/AgClO_4$ reference electrode. The m-DNB concentration was .02 M and the rotation speed was 300 rpm. Two steps in the reduction are clearly visible and marked by limiting currents at 27 microamps and 46 microamps for the first and second waves, respectively. These occur at -1.57 volts and -2.25 volts.

Figure 10 shows the voltage-current curves for four different rotation speeds on the electrode in .0381 M m-DNB. The potentials in this case are measured versus the platinum counter electrode. The voltage drop due to solution resistance has not been subtracted from the data. It can be seen that the limiting currents for the two waves increase with rotation speed.

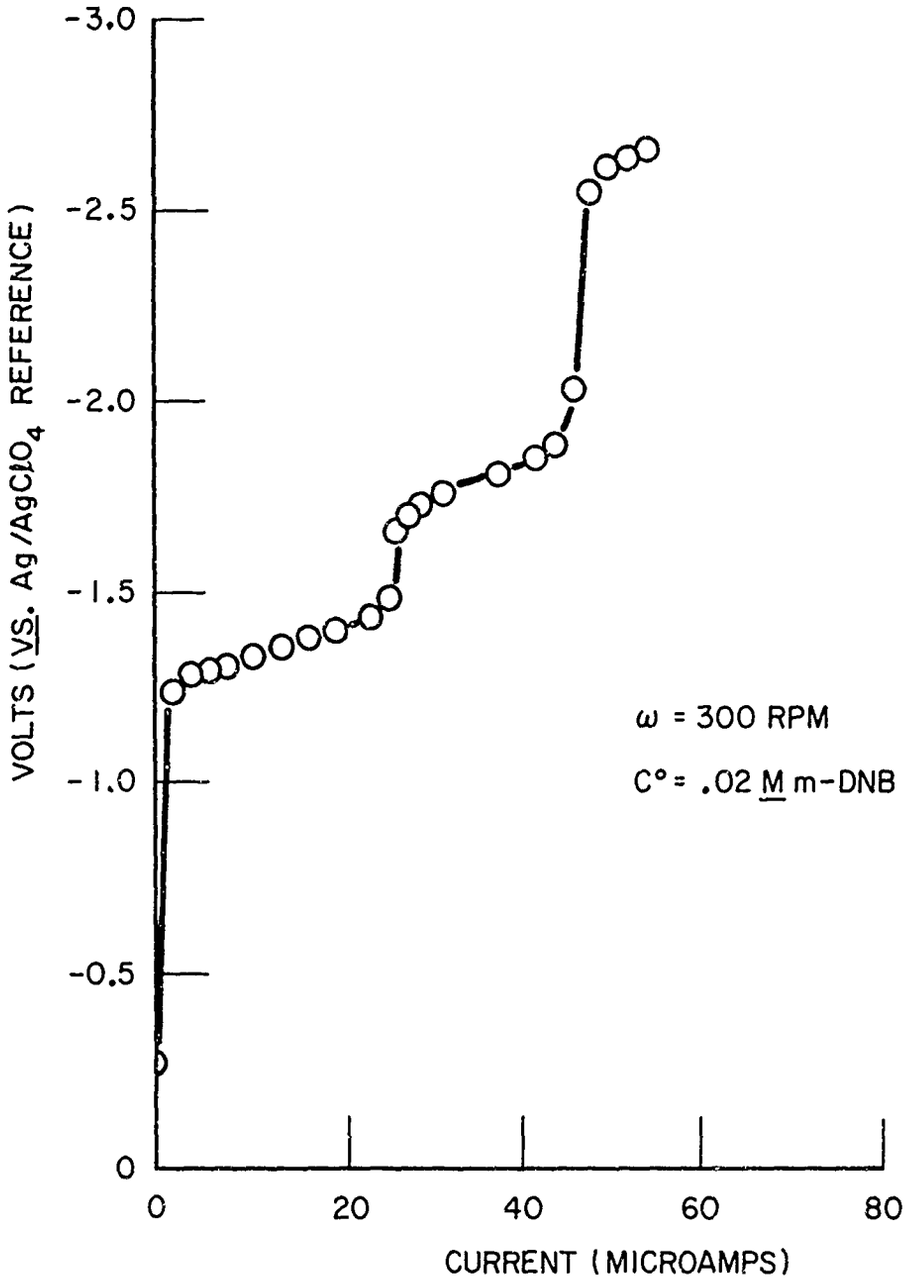

CURRENT–VOLTAGE CURVE FOR REDUCTION OF m–DNB IN THE ABSENCE OF PROTON DONORS ON THE ROTATING DISK ELECTRODE

Figure 9

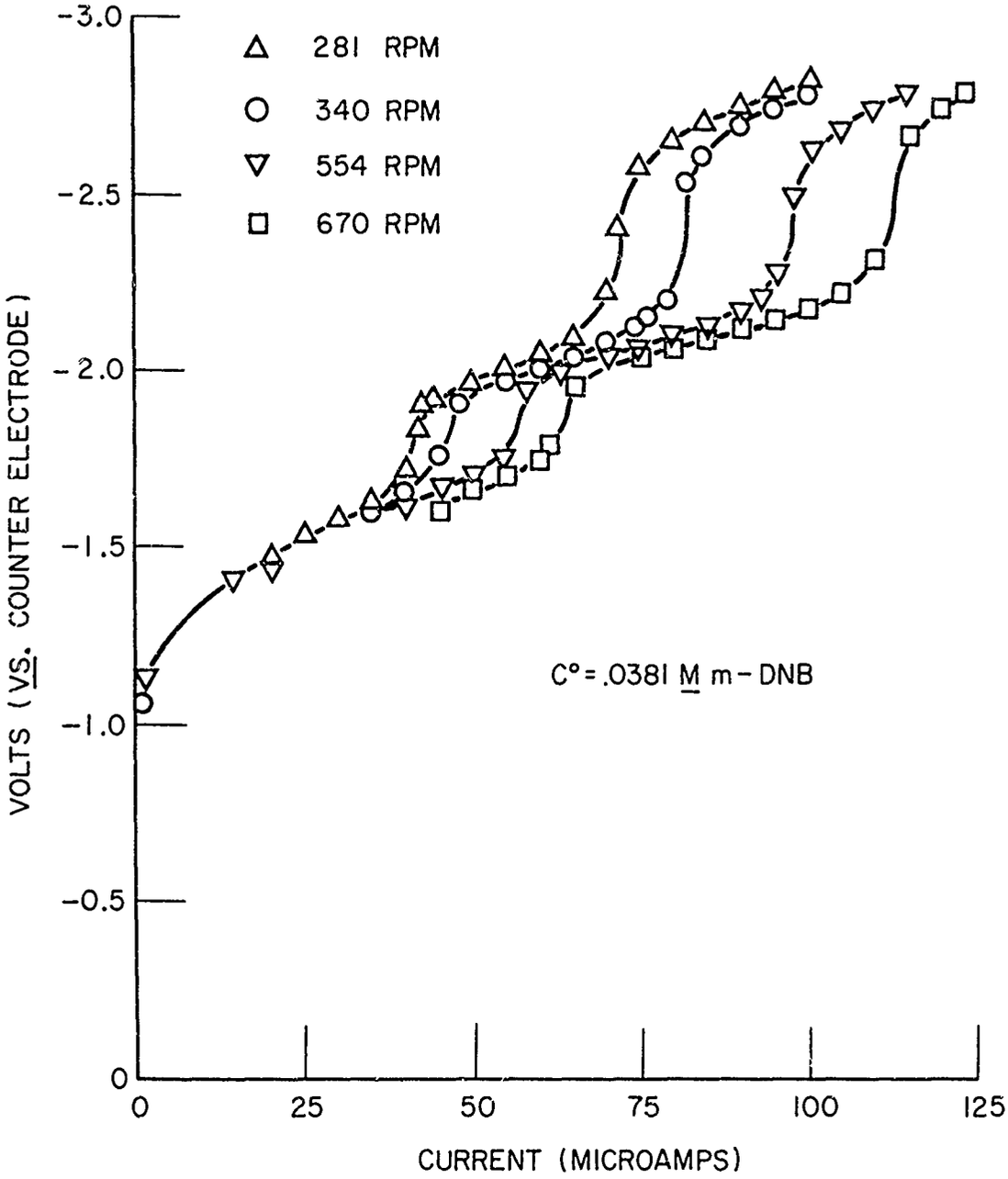

CURRENT–VOLTAGE CURVES AS A FUNCTION OF ROTATION SPEED FOR m–DNB IN DMSO IN THE ABSENCE OF PROTON DONORS

Figure 10

The dependence of the limiting currents for the first and second waves on the square root of the rotation speed (in radians/second) is shown in Figures 11 and 12 for different concentrations of m-DNB. These figures show the linear dependence, predicted by Equation (1), for the range of rotation speed and concentration investigated. Figures 13 and 14 show the dependence of the quantity $i_l/\omega^{\frac{1}{2}}$ on the bulk concentration of m-DNB. These also show a linear dependence, as indicated by Equation (1), with slopes as follows:

1st wave: $$\frac{i_l}{\omega^{\frac{1}{2}} C^o} = 0.205 \quad \frac{\text{coul cm}^3}{\text{mole sec}^{\frac{1}{2}}} \tag{25}$$

2nd wave: $$\frac{i_l}{\omega^{\frac{1}{2}} C^o} = 0.358 \quad \frac{\text{coul cm}^3}{\text{mole sec}^{\frac{1}{2}}} \tag{26}$$

Using Equation (1) and the values of the diffusion coefficient and kinematic viscosity presented earlier, an effective, overall number of electrons transferred per mole of m-DNB can be calculated for each reduction step. For the first step the value found was $n = 1.01 \pm .1$. For the second step the value is $n = 1.76 \pm .1$.

The use of Equation (1) assumes that the flow regime is laminar. This can be achieved up to Reynolds numbers of 10^4 with well balanced disks. The Reynolds number, given by,

$$Re = \frac{u_e D_e}{\nu} = \frac{D_e^2}{2\nu} \omega \tag{27}$$

was calculated to be 240 based on the diameter of the working electrode and was 2250 based on the diameter of the whole disk for the maximum rotational speed used. This is well within the laminar flow regime. Levich[14] also assumes that the thickness of the hydrodynamic boundary layer, given by,

$$\delta_o = 3.6\sqrt{\frac{\nu}{\omega}} \tag{28}$$

is much smaller than the diameter of the disk. This enables one to neglect the effects of the edge of the disks on the solution to the Navier-Stokes equations. For the lowest rotational speed used, δ_o was calculated to be .085 cm, which is small compared to the radius of the disk

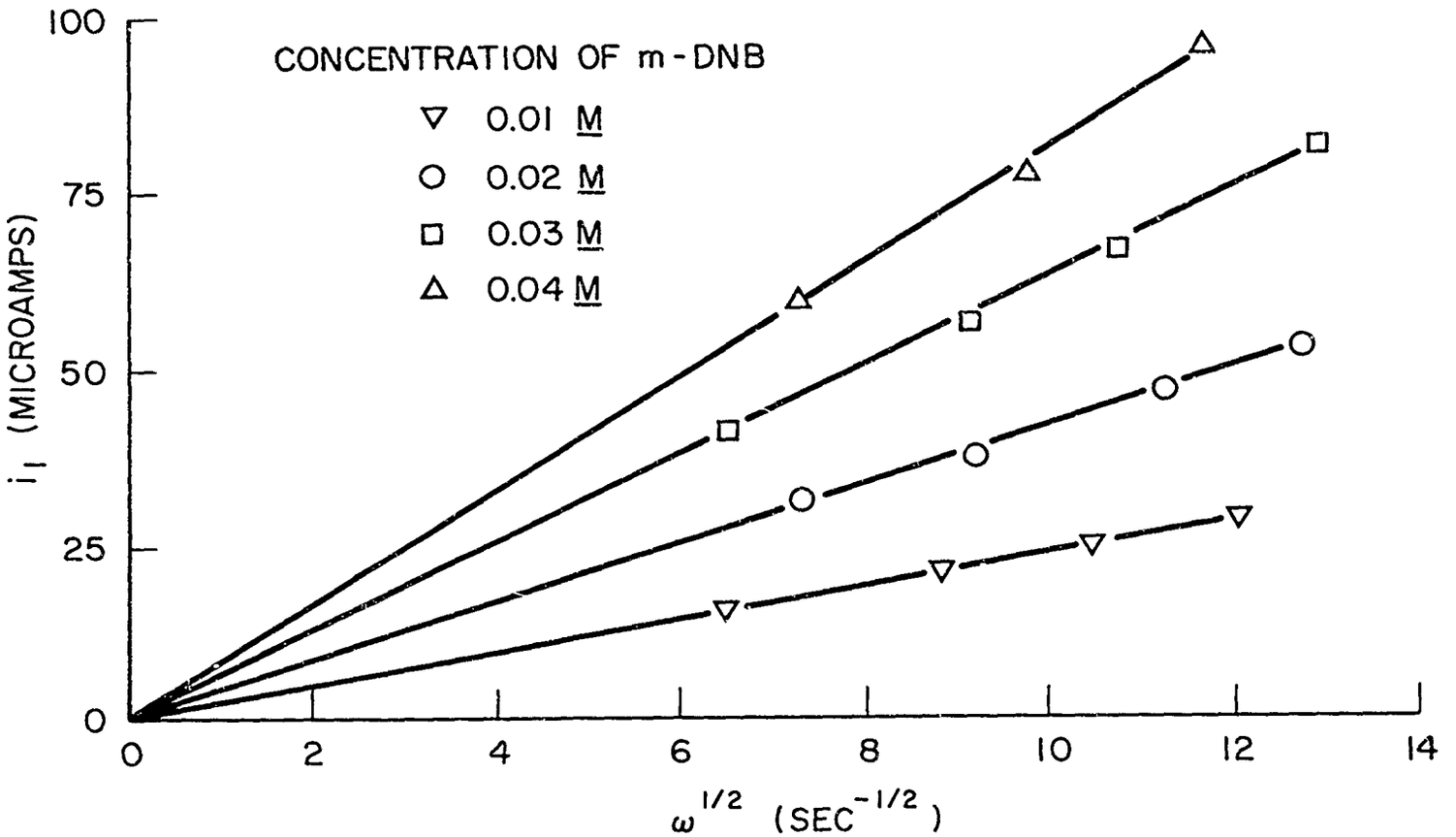

LIMITING CURRENT DEPENDENCE ON $\omega^{1/2}$ FOR 1st WAVE IN THE ABSENCE OF PROTON DONORS

Figure 11

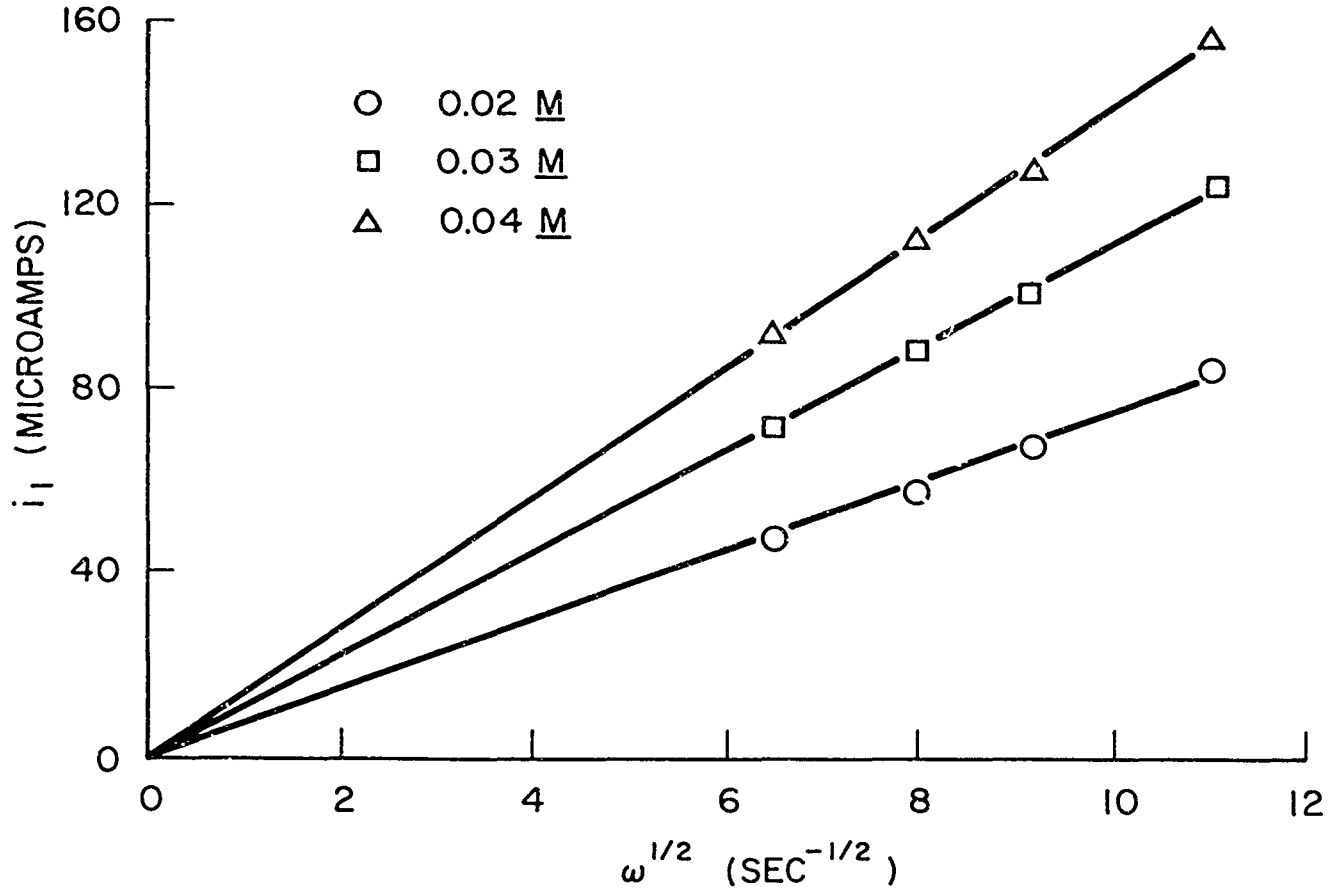

LIMITING CURRENT DEPENDENCE ON $\omega^{1/2}$ FOR 2nd WAVE IN THE ABSENCE OF PROTON DONORS

Figure 12

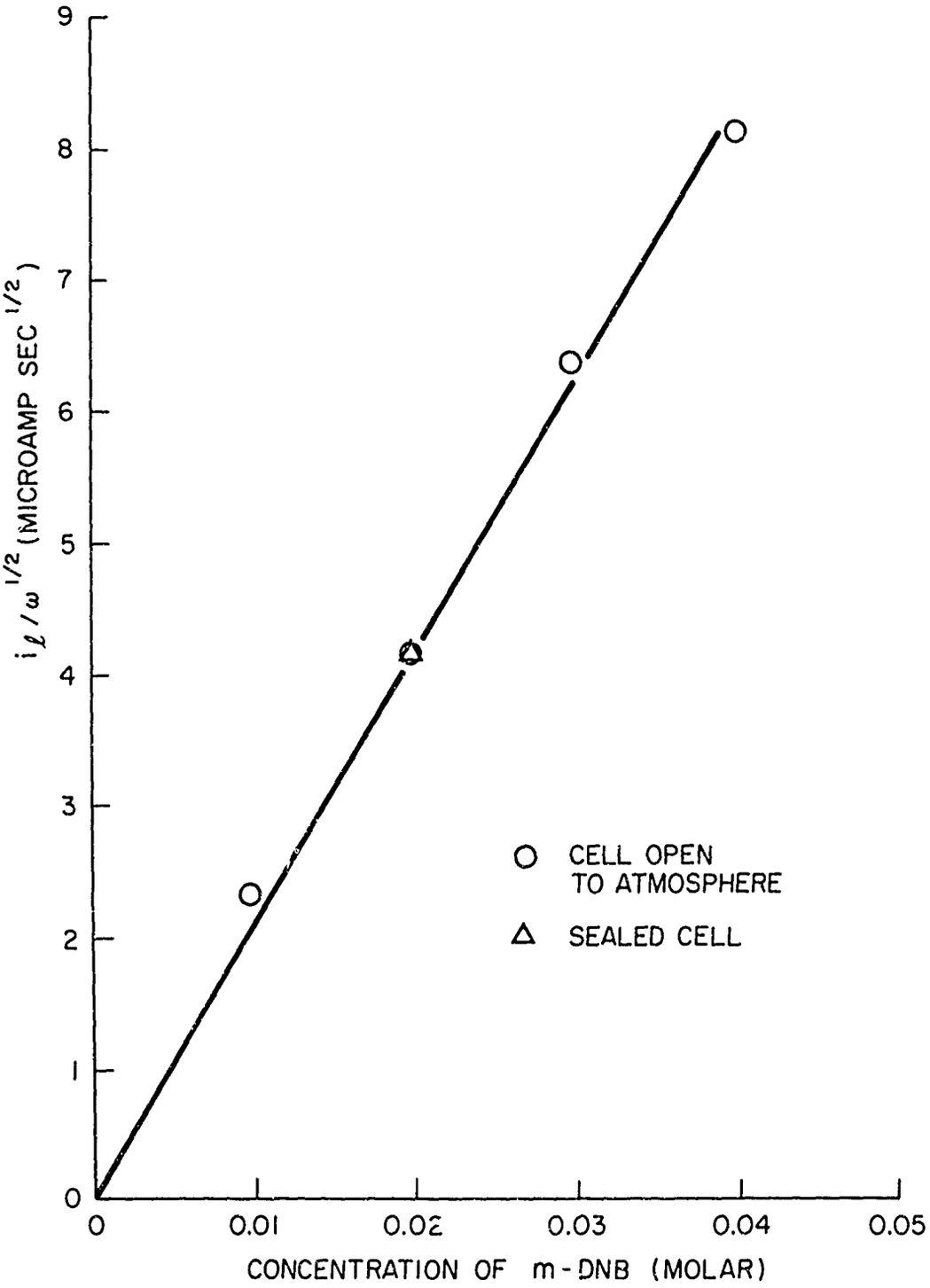

DEPENDENCE OF $i_\ell/\omega^{1/2}$ ON CONCENTRATION OF m–DNB IN THE ABSENCE OF PROTON DONORS. FIRST WAVE.

Figure 13

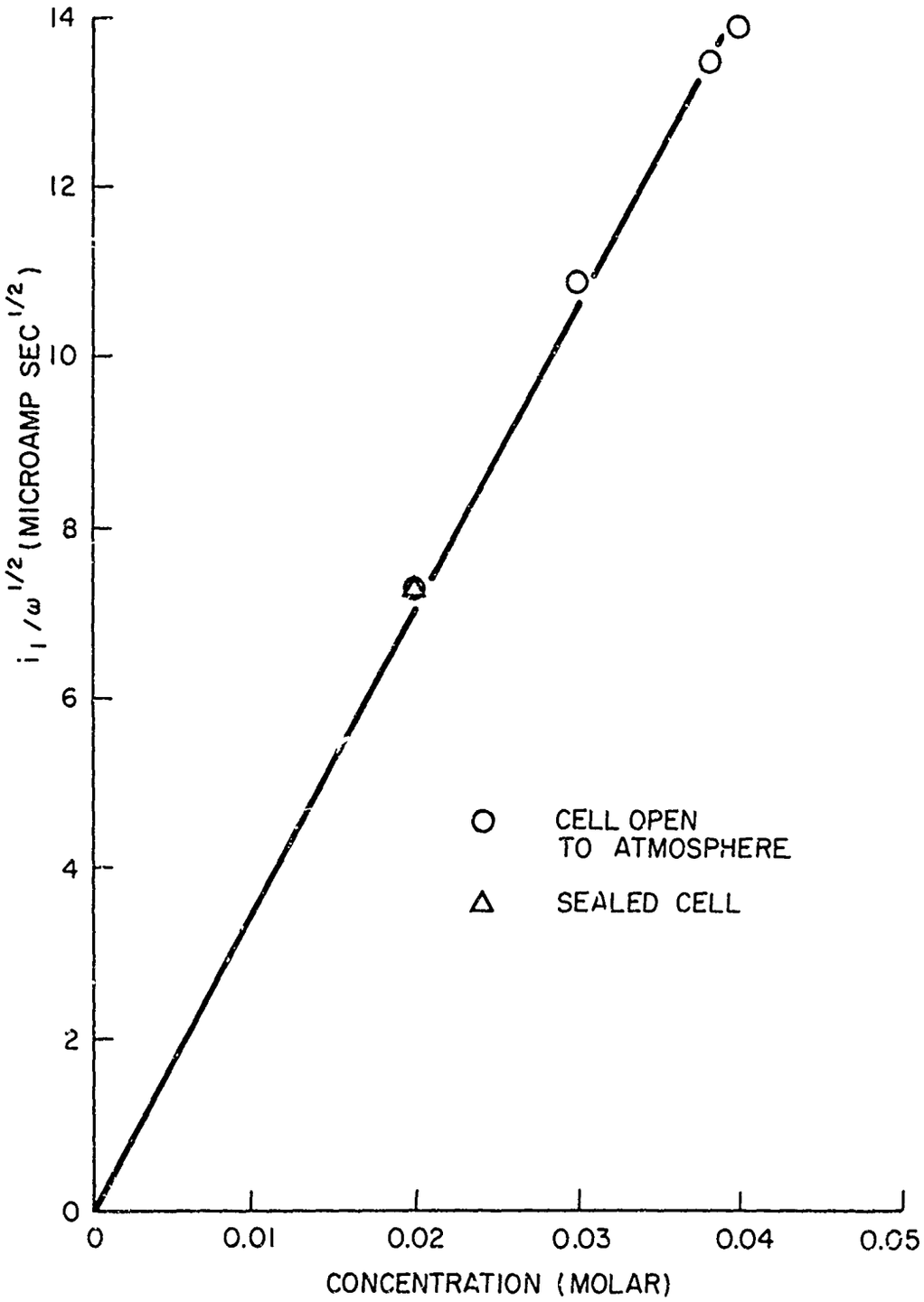

DEPENDENCE OF $i_1/\omega^{1/2}$ ON CONCENTRATION OF m–DNB IN THE ABSENCE OF PROTON DONORS. SECOND WAVE.

Figure 14

An additional assumption is that the diffusion boundary layer thickness given by

$$\delta = 1.61 \left(\frac{D}{\nu}\right)^{\frac{1}{3}} \frac{\nu}{\omega} \tag{29}$$

is small compared with the hydrodynamic boundary layer thickness. For the values of D and ν used in this experiment, δ/δ_o was calculated to be 0.03, which justifies this assumption.

When ammonium perchlorate was added to the electrochemical cell in which the rotating disk was placed, the characteristic red color of the product of the first wave seemed to fade. At higher concentrations of ammonium perchlorate the red color was not observed at all. The reduction of the ammonium ion appeared to interfere with the second wave of the m-DNB reduction. Because of this interference only the effect of NH_4^+ addition on the first wave was considered in this study.

The addition of the NH_4^+ ion to the test solutions had a marked effect on the limiting currents observed. The quantity R_d is defined as the ratio of the concentration of the ammonium perchlorate to the concentration of m-DNB in solution. In these experiments the m-DNB concentration was held constant at .02M while the NH_4^+ concentration was increased by adding ammonium perchlorate. Figure 15 shows the effect of increasing R_d on the reduction of m-DNB. As R_d is increased, the limiting current also increases. Figure 16 shows the effect of increasing R_d on the limiting current of the first wave. At values of R_d below approximately three, the limiting current is proportional to R_d. Above this value, the limiting current is insensitive to R_d.

It is interesting to note from Figure 16 that the addition of NH_4^+ ion causes the effective number of electrons transferred in the first wave to increase from 1.0 to about 3.46 per molecule of m-DNB in the bulk of the solution. The significance of these numbers are discussed in the section "Interpretation of Results."

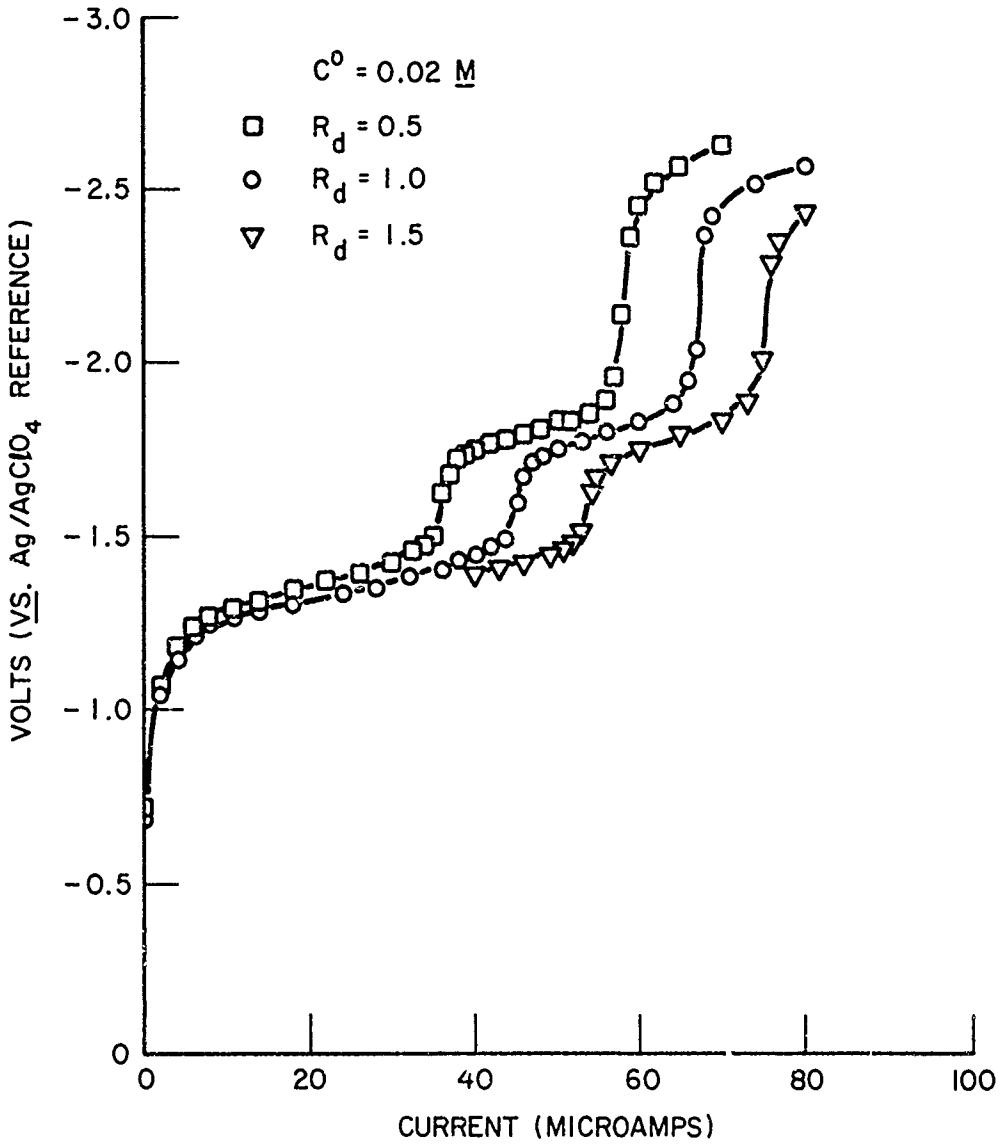

CURRENT–VOLTAGE CURVES FOR m–DNB REDUCTION AS A FUNCTION OF PROTON DONOR CONCENTRATION

Figure 15

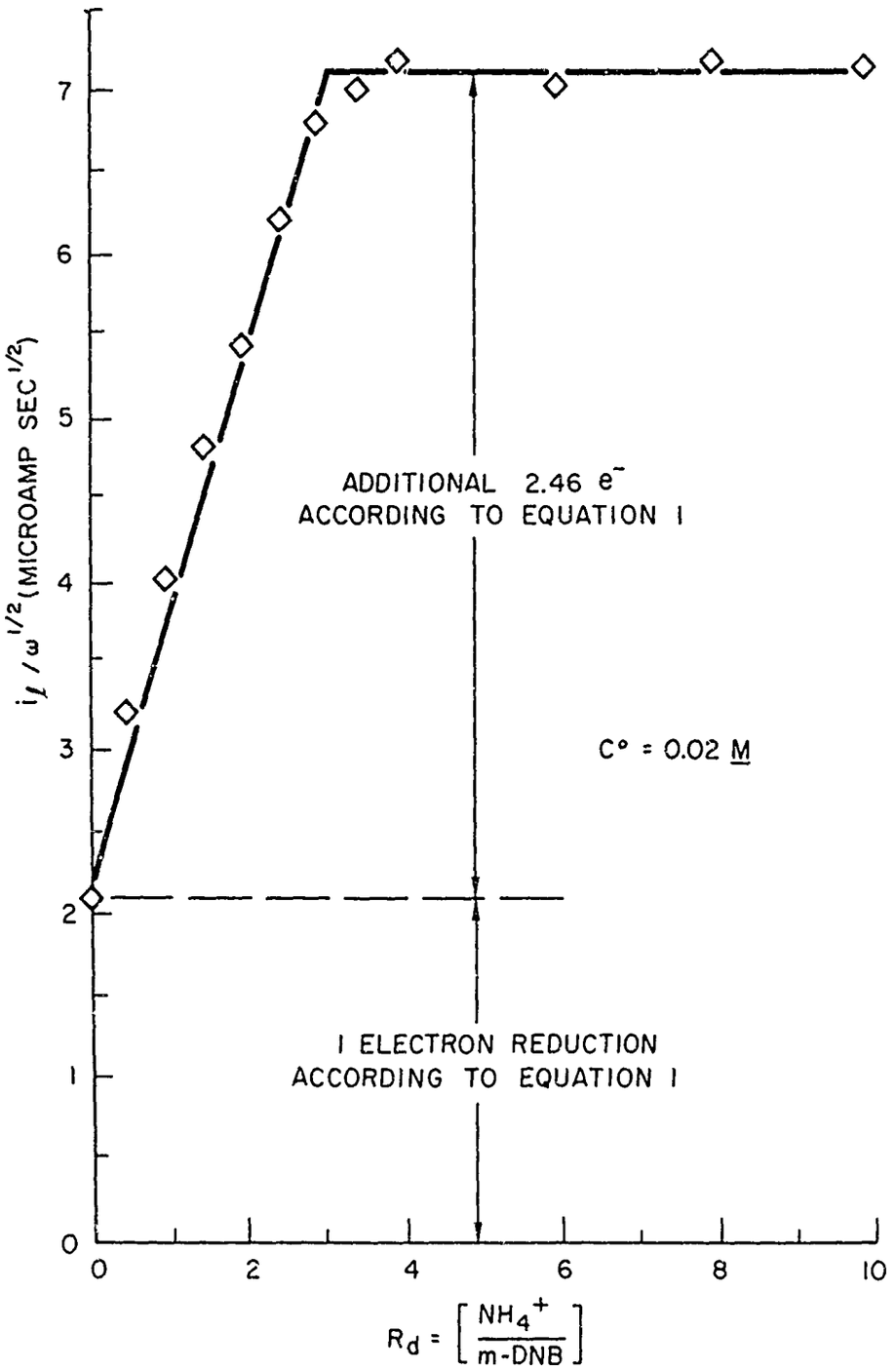

THE EFFECT OF ADDITION OF AMMONIUM PERCHLORATE ON THE 1st WAVE REDUCTION OF m–DNB IN DMSO

Figure 16

4. Potential Step. The application of a potential step to the platinum sphere electrode in a solution of m-DNB in 0.1 M TEAP-DMSO caused the appearance of a soluble red substance at the surface of the electrode. The physical appearance of the substance was the same as that observed for the rotating disk experiments.

Figures 17 and 18 are plots of the observed current versus the inverse of the square root of the time from the application of the potential step. Figure 17 results from the application of -1.7 volts versus the counter electrode. This corresponds to the first step of the reduction of m-DNB. Figure 18 represents the second step in the reduction of m-DNB, due to the application of a voltage step of -2.3 volts versus the counter electrode. It is clear that, for times between 0.2 and 2.0 seconds, the plots are linear and pass nearly through zero for each concentration investigated. This indicates that the conditions of the experiment are such that Equation (6) can be applied.

Figure 19 shows the dependence of the slopes of Figure 17 and 18 on the concentrations used. It can be seen that the slopes are proportional to the bulk concentration of m-DNB, as predicted by Equation (6). This is true for both the first and second steps. The slopes of the lines in Figure give the following quantities:

$$\text{1st step} \qquad \frac{i\,t^{\frac{1}{2}}}{c^{o}} = 10.9 \qquad \frac{\text{amp sec}^{\frac{1}{2}}\ \text{cm}^{3}}{\text{mole}} \tag{30}$$

$$\text{2nd step} \qquad \frac{i\,t^{\frac{1}{2}}}{c^{o}} = 19.7 \qquad \frac{\text{amp sec}^{\frac{1}{2}}\ \text{cm}^{3}}{\text{mole}} \tag{31}$$

Using Equation (6), the value of the diffusion coefficient previously determined, and the area of the electrode, effective overall numbers of electrons transferred were calculated. They are:

$$\begin{aligned} &\text{1st step} \quad n = .95 \pm .1 \\ &\text{2nd step} \quad n = 1.71 \pm .1 \end{aligned} \tag{32}$$

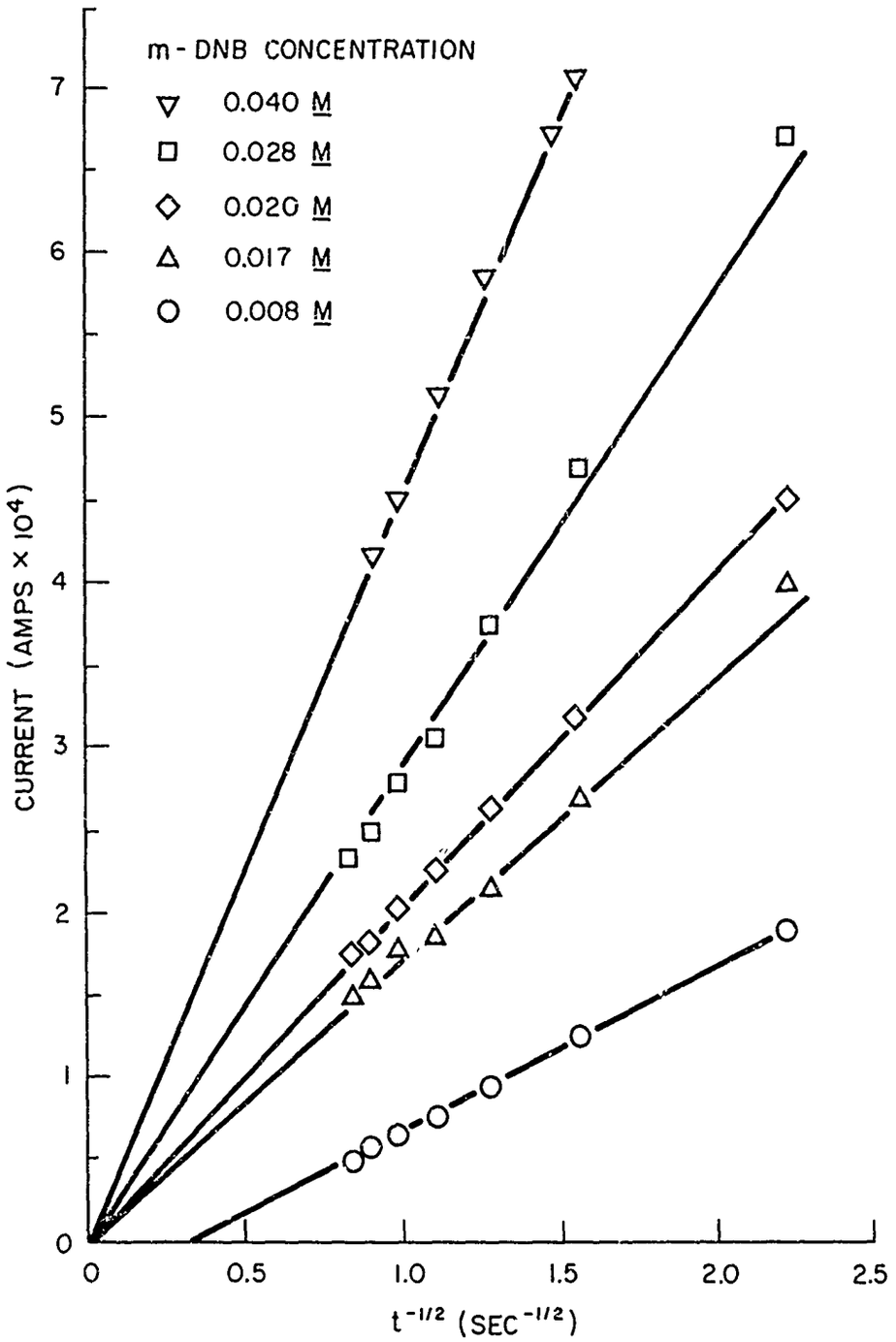

CURRENT VS. TIME$^{-1/2}$ FOR 1st WAVE REDUCTION OF m–DNB IN DMSO IN THE ABSENCE OF PROTON DONORS FROM THE POTENTIAL STEP METHOD

Figure 17

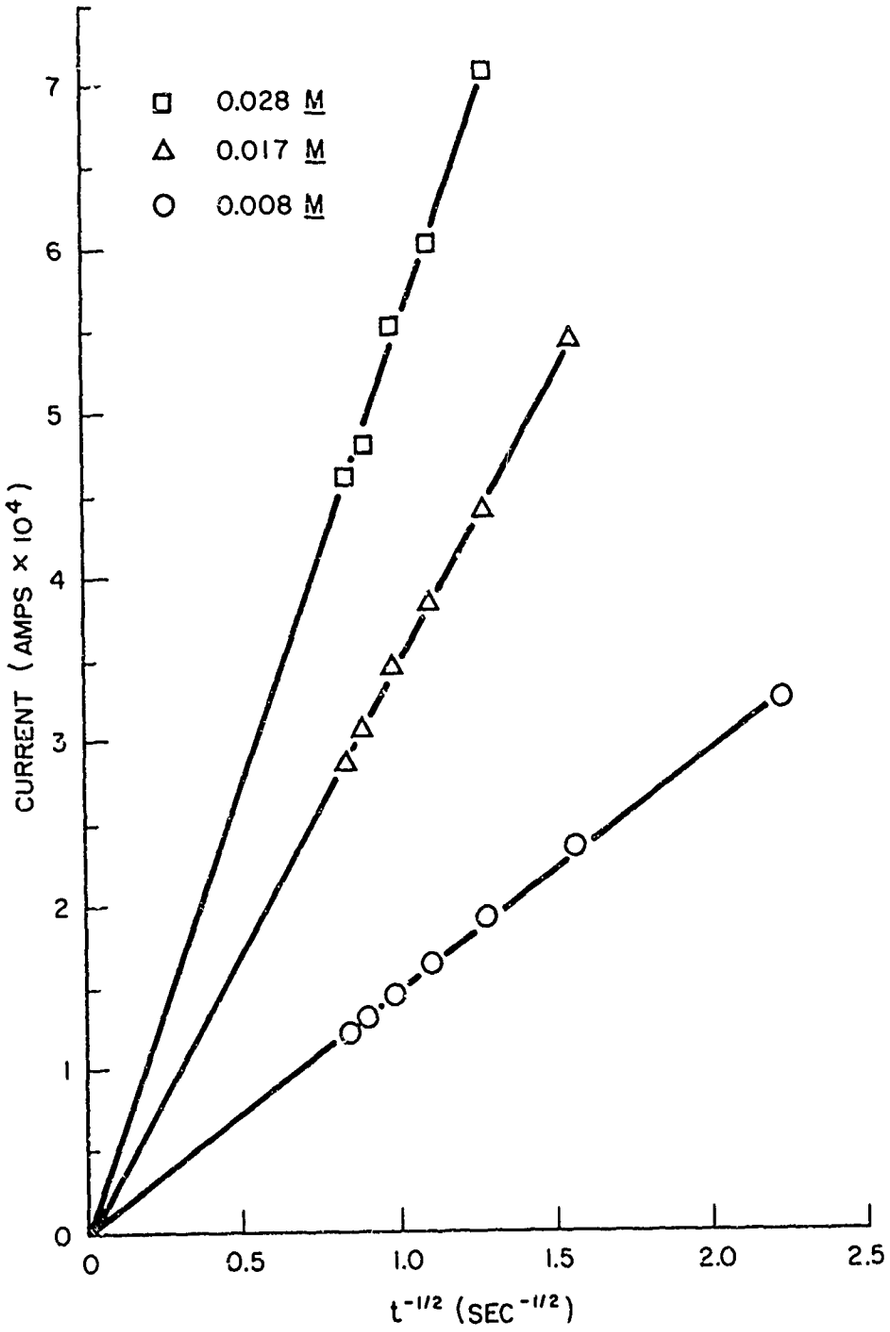

CURRENT VS. TIME$^{-1/2}$ FOR 2nd WAVE REDUCTION OF m–DNB IN DMSO IN THE ABSENCE OF PROTON DONORS FROM THE POTENTIAL STEP METHOD

Figure 18

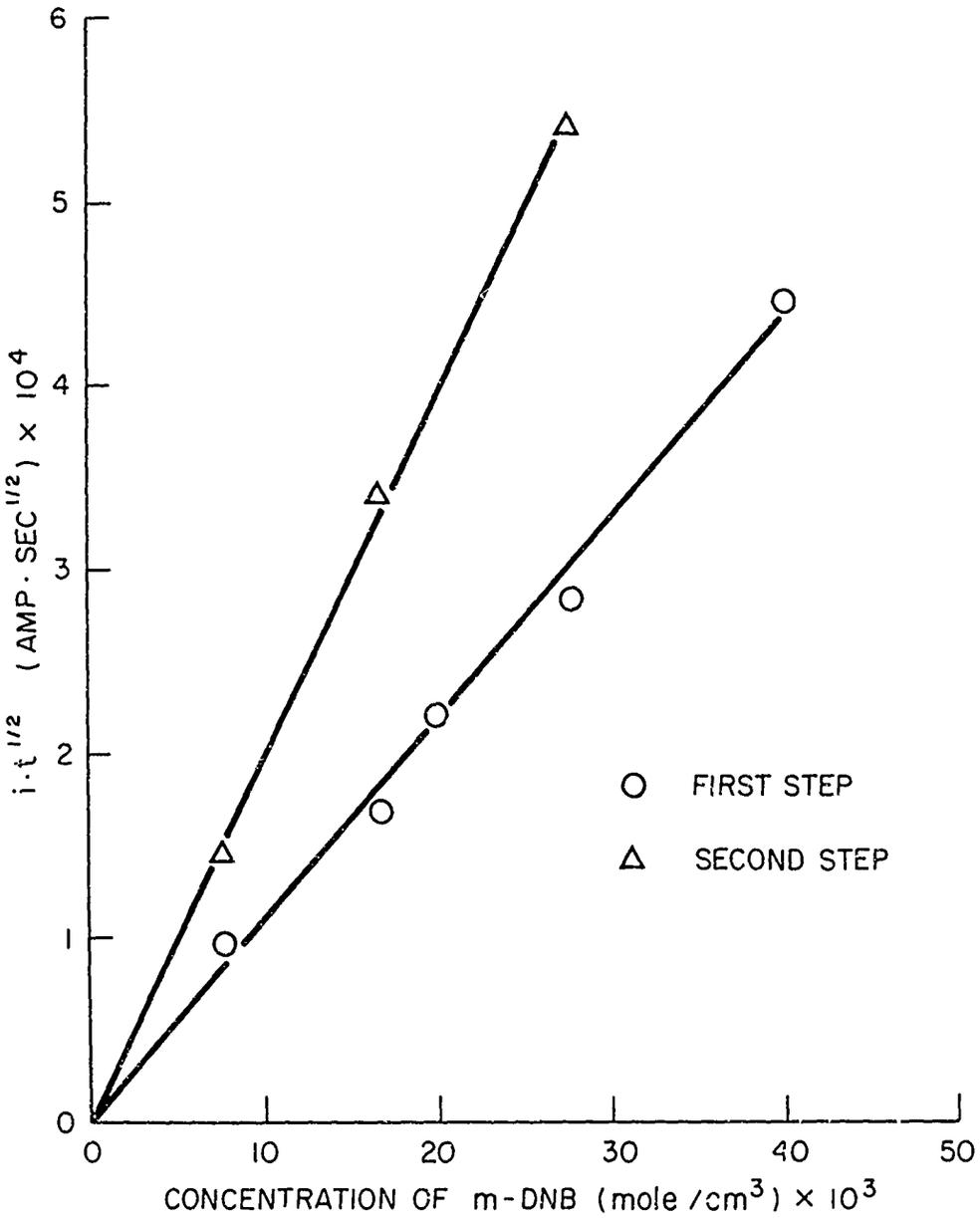

CONCENTRATION DEPENDENCE OF THE QUANTITY $i \cdot t^{1/2}$ FOR 1st AND 2nd WAVES IN REDUCTION OF m–DNB IN THE ABSENCE OF PROTON DONORS FROM THE POTENTIAL STEP METHOD

Figure 19

The maximum time at which data was taken was two seconds. Equation (6) assumes that the solution in the cell is stagnant. Another way of saying this is that the diffusion boundary layer on the electrode must be much smaller than the hydrodynamic boundary layer caused by natural convection. Delahay[17] gives the concentration as a function or r and t as:

$$\frac{C(r,t)}{C^o} = 1 - \frac{r_o}{r} \operatorname{erfc} \frac{r-r_o}{2D^{\frac{1}{3}}t^{\frac{1}{2}}} \tag{33}$$

where r_o is the radius of the electrode (0.0825 cm in the present case). Figure 20 shows the concentration ratio above as a function of the distance from the surface of the electrode, at a time two seconds after the application of the potential step. The diffusion boundary layer thickness, δ, can be defined by:

$$\left[\frac{\partial\left(\frac{C}{C^o}\right)}{\partial r}\bigg|_{r=r_o}\right](\delta - r_o) = 1 \tag{34}$$

From Equation (34), δ was calculated to be 6.2×10^{-3} cm after 2 seconds. At this point the concentration of m-DNB is approximately 82% of the bulk concentration. No convection was observed in the cell until many minutes after the application of the potential step. This was due to the fact that the difference in density between the products and the reactants was very small. Also, the total currents involved were quite small (on the order of .1 milliamp) so that very little of the product material was formed. It may be concluded from these observations that convection was not important during the time range investigated.

5. Interpretation of Results. The results of the potential step experiments and the rotating disk electrode experiments are in good agreement. It is clear that the first step in the reduction of m-DNB in .1M TEAP-DMSO results from a single electron transfer. This observation is in good agreement with the conclusions of other investigators of nitro-compound reductions.

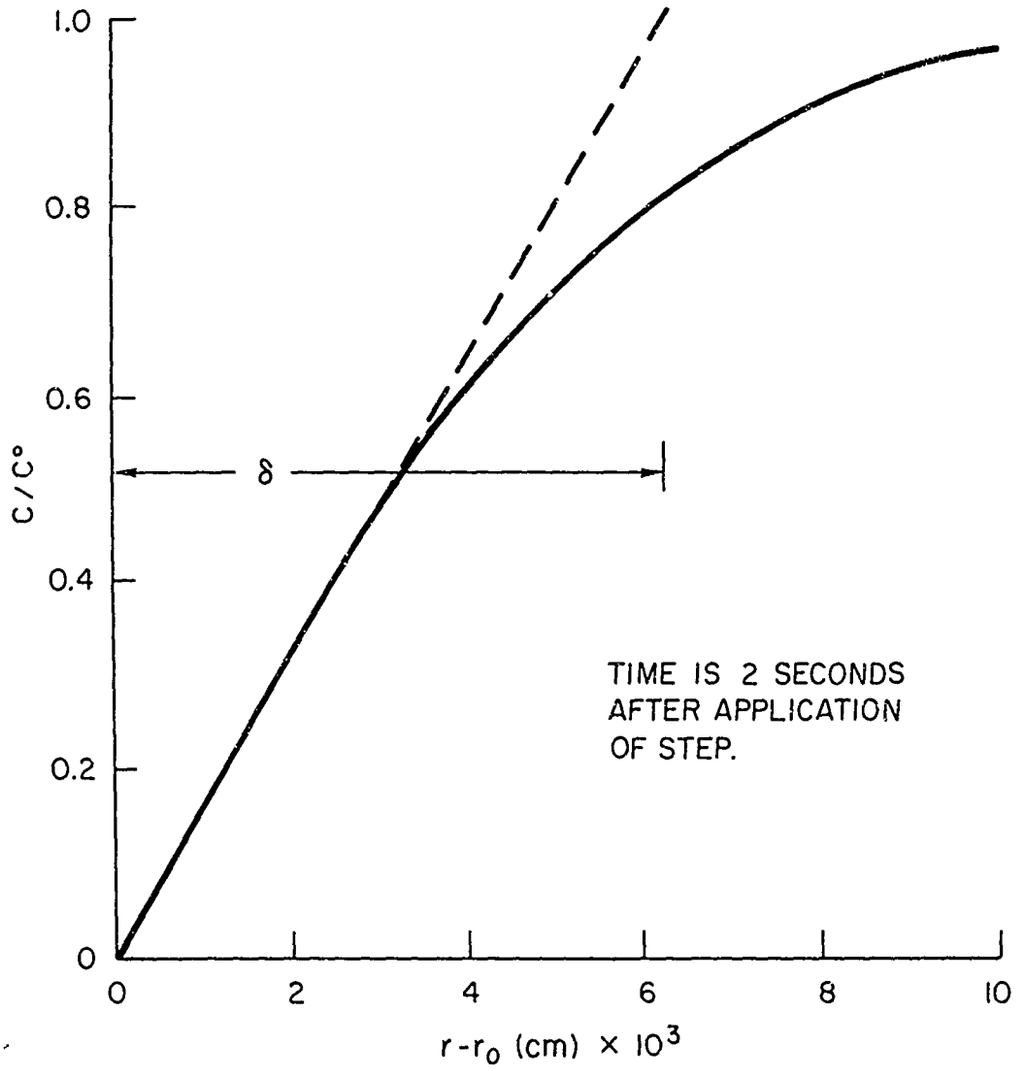

CALCULATED CONCENTRATION PROFILE FOR m–DNB FOR THE POTENTIAL STEP METHOD

Figure 20

The second step yields an effective, overall number of electrons of about 1.75 per molecule of m-DNB in the bulk of the solution. The second step therefore, adds an effective .75 electrons to the radical anion produced by the first step. If the second step is also a one electron transfer, this suggests that only 75% of the radical anion produced by the first step is reacted in the second step.

Kemula and Sioda[10] found for nitrobenzene that the second wave height of the reduction in dimethylformamide was less than proportional to the concentration of nitrobenzene at concentrations greater than 3.5×10^{-4}M. In all probability, considering the general reaction system of Hoijtink,[32] the second wave is the reduction of the radical anion to the di-negative state. The fact that less than one electron seems to be involved may be due to a complicated mechanism involving desorption and/or reaction with the solvent which is not yet fully understood.

The possibility that the second wave somehow involves an attack on the second nitro-group of m-DNB is not excluded by the above remarks. However, it is to be noted that the second wave has been observed for nitrobenzene[10] and other mono-nitrocompounds[13] where the second nitro-group is not present to be attacked. Thus, it seems that the formation of the radical di-anion is quite reasonable in this case.

The effect of the addition of ammonium perchlorate on the reduction of m-DNB appears to correspond to the behavior reported by Given and Peover[8] as class C, involving the protonation of the radical anion formed by the first electron transfer. The first reduction step in the absence of a proton donor produced a red substance in both the potentiostatic step and rotating disk experiments. This corresponds to the formation of the m-DNB radical anion. If the radical anion disappears by reaction in solution upon addition of proton donors, one would expect the color to disappear also. The observed loss of red color upon addition of ammonium ions may thus be considered evidence that a reaction, such as protonation, occurs.

A detailed mechanism, corresponding to class C behavior of Given and Peover was proposed by Koopmann and Gerischer[23] for the reduction of nitrobenzene in weakly alkaline aqueous solutions. By applying this mechanism to the case under consideration here, the following system of reactions is proposed:

$$\left(\phi_{NO_2}^{NO_2}\right)_{SOLN} \rightleftharpoons \left(\phi_{N\phi_2}^{NO_2}\right)_{ADS} \qquad \text{I}$$

$$\left(\phi_{NO_2}^{NO_2}\right)_{ADS} + \bar{e} \rightleftharpoons \left(\cdot\,\phi_{NO_2}^{NO_2^-}\right)_{ADS} \qquad \text{II}$$

$$\left(\phi_{NO_2}^{NO_2}\right)_{ADS} \rightleftharpoons \left(\cdot\,\phi_{NO_2}^{NO_2^-}\right)_{SOLN} \qquad \text{III}$$

$$\left(\phi_{NO_2}^{NO_2^-}\right)_{SOLN} + NH_4^+ \rightleftharpoons \phi_{NO_2}^{NO_2H} + NH_3 \qquad \text{IV}$$

$$\phi_{NO_2}^{NO_2H} + \left(\cdot\,\phi_{NO_2}^{NO_2^-}\right)_{SOLN} \rightleftharpoons \phi_{NO_2}^{NO} + (OH)^- \qquad \text{V}$$

$$\phi_{NO_2}^{NO} + \left(\cdot\,\phi_{NO_2}^{NO_2^-}\right)_{SOLN} + NH_4^+ \rightleftharpoons \phi_{NO_2}^{NOH} + \phi_{NO_2}^{NO_2} + NH_3 \qquad \text{VI}$$

$$\phi_{NO_2}^{NOH} + \left(\cdot\,\phi_{NO_2}^{NO_2^-}\right)_{SOLN} + NH_4^+ \rightleftharpoons \phi_{NO_2}^{NHOH} + \phi_{NO_2}^{NO_2} + NH_3 \qquad \text{VII}$$

It can be seen that the radical amion formed by reaction II serves to transfer electrons in the solution reactions IV and VII. The completion of reaction VII requires reaction II to take place four times, providing four radical anions. Thus the system of reactions above can be condensed, neglecting the effect of the desorption reactions I and III, into the following heterogeneous and homogeneous reactions:

$$4\ \phi_{NO_2}^{NO_2} + 4\bar{e} \rightleftharpoons 4 \cdot \phi_{NO_2}^{NO_2^-} \qquad \text{VIII}$$

$$4 \cdot \phi_{NO_2}^{NO_2^-} + 3\,NH_4^+ \rightleftharpoons \phi_{NO_2}^{NHOH} + 3\,\phi_{NO_2}^{NO_2} + 3\,NH_3 + (OH) \qquad \text{IX}$$

The overall reaction becomes:

$$\phi_{NO_2}^{NO_2} + 4\bar{e} + 3\,NH_4^+ \rightleftharpoons \phi_{NO_2}^{NHOH} + 3\,NH_3 + (OH^-) \qquad \text{X}$$

Equation X predicts that the stoichiometric ratio of NH_4^+ ions to m-DNB in the solution is 3 to 1. Experimentally, this is confirmed by Figure 16 which shows the current increasing with NH_4^+ concentration up to a point where the 3 to 1 ratio is reached. At this point the ammonium ion concentration no longer limits the current and the current therefore becomes independent of NH_4^+ concentration.

Equation (1), which was used to predict the number of electrons transferred as a function of the limiting current, was derived for the case in which no chemical reactions were taking place in solution. Equation IX represents just such a reaction and, consequently, Equation (1) must be modified to account for this.

In order to modify Equation (1) one must solve the continuity equations for each species of interest. In this case these species are m-DNB and the radical anion. It will be assumed that the reaction represented by Equation IX is fast enough that all reaction takes place within the diffusion layer. In this case the species equations become:

$$\frac{dC_1}{dt} = 0 = D\frac{d^2C_1}{dx^2} + \frac{3}{4}\,k\,C_2 \qquad (35)$$

$$\frac{dC_2}{dt} = 0 = D\frac{d^2C_2}{dx^2} - k\,C_2 \qquad (36)$$

where C_1 and C_2 are the concentrations of m-DNB and the radical anion, respectively.

In writing Equations (35) and (36) it has been assumed that the diffusion coefficients for the two species are equal and independent of concentration. It has also been assumed that the reaction IX is first order with respect to the radical anion, and that there is enough NH_4^+ present that it does not limit the current, as discussed above.

The boundary conditions of Equations (35) and (36) are as follows. On the surface of the electrode the concentration of the m-DNB is zero due to the assumption of diffusion limited current. In addition the flux of the m-DNB approaching the electrode is just equal to the flux of the radical anion leaving the electrode. These conditions may be summarized as follows:

at the surface

$$C_1 = 0$$
$$|j_1| = |j_2| = i_1/FA \tag{37}$$

in the bulk of the solution (a distance δ away from the electrode)

$$C_1 = C^o$$
$$C_2 = 0 \tag{38}$$

The solutions of the equations for C_1 and C_2 are:

$$C_1 = C^o \quad 1 - \left(\frac{3 \sinh \lambda x + \lambda x \cosh \lambda\delta}{3 \sinh \lambda\delta + \lambda\delta \cosh \lambda\delta}\right) \tag{39}$$

$$C_2 = C^o \left(\frac{\sinh \lambda x}{\sinh \lambda\delta}\right) \left[\frac{1}{\frac{3}{4} \lambda\delta \sinh \lambda\delta + \frac{1}{4} \lambda^2 \delta^2 \cosh \lambda\delta}\right] \tag{40}$$

where

$$\lambda \equiv \sqrt{\frac{k}{D}} \tag{41}$$

If the above equations are solved for the limiting current, the resulting relation is:

$$i_{lim} = \left[\frac{1}{\frac{1}{4} + \frac{3}{4} \frac{1}{\lambda\delta} \tanh \lambda\delta} \right] \frac{FADC^{o}}{\delta} \tag{42}$$

It is interesting to note that the quantity in brackets in Equation (42) corresponds to the "number of electrons" which would be observed for Equation (1). At low reaction rates, where $\lambda\delta$ is small, this quantity approaches unity, the true number of electrons transferred per electrode reaction. At high rates of homogeneous reaction, the value gives the equivalent of a four electron reduction.

It is clear that the rate of reaction IX has a dependence on the nature of the proton donor and its ability to donate a proton in DMSO . 1M TEAP solutions. It is expected that strong proton donors would give a high rate constant while relatively weak donors, like the ammonium ion, would give somewhat smaller rate constants. If the value of the limiting current of 3.46 electrons from Figure 16 is substituted for the quantity in brackets in Equation 42 an overall rate constant can be calculated to be:

$$k = 2.5 \text{ sec}^{-1}$$

In acid solutions the OH^- ion produced by reaction V would probably be reacted with another proton donor so that a ratio of 4 to 1 for proton donor concentration to active species concentration would be observed. This appears to be the case for benzoic acid in dimethylformamide in the reduction of nitrobenzene studied by Kemula and Sioda.[10]

CONCLUSIONS

The reduction of m-DNB in DSMO at a platinum electrode in the absence of a proton donor takes place in two distinct steps. The first step corresponds to a one electron transfer and may be postulated to be the formation of the m-DNB radical anion by comparison with the results of Kemula and Sioda.[10] The second step, occurring at more negative potentials than the first, involves less than one electron, overall. It is assumed that this step is actually a one electron reduction of the radical anion. This explanation is in accord with Hoijtink's[7] general mechanism for hydrocarbon reduction.

In the presence of ammonium perchlorate, a proton donor, the results of the experiments performed are consistent with the following mechanism. The radical anion formed by the first wave reduction reacts in solution with the ammonium ion in a complex series of reactions similar to those proposed by Koopmann and Gerischer[23] for nitrobenzene reduction. In this way the radical anion acts as the charge transfer agent in solution. The formation of nitro-phenyl-hydroxylamine as a product, and an overall transfer of four electrons is consistent with the mechanism proposed for the first wave in the presence of a proton donor.

A reaction rate constant for the homogeneous protonation reaction in the range of 22-24°C was calculated to be 2.5 sec.$^{-1}$ by the application of the species conservation equations to the experimental data.

The use of the rotating disk technique to investigate problems involving homogeneous reactions of electrode reaction products enables one to analyze a rather complicated reaction scheme. The greatest uncertainties in the use of this technique are those in the determination of the diffusion coefficient. The potential step technique for single electron transfers provides a good check on the rotating disk technique, but is burdened with time dependent equations for more complicated systems.

PRECEDING PAGE BLANK

BIBLIOGRAPHY

1. Jasinski, Raymond, *High Energy Batteries*, Plemun Oress, New York, 1967.

2. Yao, N.P., E. d'Orsay, and D.N. Bennion, "Nonaqueous electrolyte systems," *U.S. Army Interim Report No. 2*, Contract No. DA-44-009-AMC-1661(T), September 1967.

3. Smyrl, W.H., "Properties of dimethyl sulfoxide as a solvent for inorganic compounds," *Internal Technical Report NOLC, Dept. of Chem. Engr. University of Calif., Berkeley*, 1963.

4. Butler, James N. "Electrochemistry in dimethyl sulfoxide," *J. Electroanal. Chem.*, *14*, 89-116 (1967).

5. Melendres, Carlos A., "Solubilities, conductances, viscosities, and densities of solutions of selected inorganic compounds in dimethylsulfoxide," *U.S. Atomic Energy Comm. Report* UCRL-16330, 1965.

6. Spindler, W.C. "A review of recently developed liquid ammonia batteries," *Proc. Advances in Battery Tech. Symposium*, *1*, 21-65 (1965).

7. Hoijtink, G.J., J. van Schooten, E. deBoer, and W. Aalbersberg, "The polarographic reduction of conjugated hydrocarbons. IV. The mechanism of the reduction of various alternant and nonalternant hydrocarbons," *Rec. Trav. Chem.*, *73*, 355-375 (1954).

8. Given, P.H. and M.E. Peover, "Polarographic reduction of aromatic hydrocarbons and carbonyl compounds in dimethylformamide in the presence of proton donors," *J. Chem. Soc., London*, 385-393, 1960.

9. Kolthoff, I.M. and T.B. Reddy, "Polarography and voltammetry in dimethylsulfoxide," *J. Electrochem. Soc.*, *108*, 980-985 (1961).

10. Kemula, W. and R. Sioda, "Polarographic reduction of nitrobenzene and nitrosobenzene in dimethylformamide," *Bull. Acad. Polon. Sci., Ser. Sci. Chim.*, *10*, 107-111 (1962).

11. Kemula, W. and R. Sioda, "Electrochemical generation and visible spectrum of nitrobenzene free radical anion in dimtehylformamide," *Nature*, *197*, 588-589 (1963).

12. Geske, D.H. and A.M. Maki, "Electrochemical generation of free radicals and their study by electron spin resonance spectroscopy; the nitrobenzene anion radical," *J. Am. Chem. Soc.*, *82*, 2671-2676 (1960).

13. Cadle, S.H., Paul R. Tice, and James Q. Chambers, "Electrochemical reduction of aromatic nitrocompounds in the presence of proton donors," *J. Phys. Chem.*, *71*, 3517-3522 (1967).

14. Levich, Veniamin G., *Physicochemical Hydrodynamics*, Prentice Hall, Englewood Cliffs, N.J., 1962.

15. Riddiford, A.C., "The rotating disk system," *Advances in Electrochemistry and Electrochemical Engineering, No. 4.* (Edited by P. Delahay and C.W. Tobias) Interscience, New York, 47-116, 1966.

16. Newman, John, "Schmidt number correction for the rotating disk," *J. Phys. Chem.*, *70*, 1327-1328 (1966).

17. Delahay, Paul, *New Instrumental Methods in Electrochemistry*, Interscience, New York, 1954.

18. Stokes, R.H., "An improved diaphragm-cell for diffusion studies, and some tests of the method," *J. Am. Chem. Soc.*, *72*, 763-767 (1950).

PRECEDING PAGE BLANK

19. Gordon, A.R., "The diaphragm cell method of measuring diffusion," *Annals of the New York Academy of Sci., 46,* 285-308 (1945).

20. Stokes, R.H., "Integral diffusion coefficients of potassium chloride solutions for calibration of diaphragm cells," *J. Am. Chem. Soc., 73,* 3527-3528 (1951).

21. Denbigh, Kenneth, *The Principles of Chemical Equilibrium,* Cambridge Univ. Press, 1964

22. Kitaigorodskii, A.J., *Organic Chemical Crystallography,* Consultants Bureau, New York, 1965, p. 365.

23. Koopmann, R. and H. Gerischer, "Untersuchung der elektrochemischen Reduktion Von Nitrobenzol durch Kombination von ESR-Messungen mit electroanalytischen Methoden," *Berichte der Bunsengesellschaft fur physikalische Chemie, 70,* 127-138 (1966).

24. Douglas, T.B., "Vapor pressure of methyl sulfoxide from 20° to 50°. Calculation of the heat of vaporization," *J. Am. Chem. Soc., 73,* 799 (1951).

25. Dunnett, J.S. and R.P.H. Gasser, "Electrolyte solutions in dimethyl sulfoxide," *Trans. Faraday Soc., 61,* 922-927 (1965).

26. Meek, D.W., D.K. Straub, and R.S. Drago, "Transition metal ion complexes of dimethyl sulfoxide," *J. Am. Chem. Soc., 82,* 6013-6016 (1960).

27. Sears, P.G., G.R. Lester. and L.R. Dawson, "A study of the conductance behavior of some univalent electrolytes in dimethyl sulfoxide at 25°," *J. Phys. Chem., 60,* 1433-1436 (1956).

28. Schlaefer, H.L. and W. Schaffernicht, "Dimethylsulfoxyd als Losungmittel fur anorganische Verbindungen," *Angewandte Chemie, 72,* 618-626 (1960).

29. Vogel, Arthur I., *A Textbook of Quantitative Inorganic Analysis,* Wiley, New York, 1961.

30. Archer, E.E. and H.W. Jeater, "Determination of small amounts of water in some organic liquids," *The Analyst,* 1965, 351-355.

31. Crown Zellerbach Corp., *Dimethyl Sulfoxide, Technical Bulletin,* 1964.

32. Crown Zellerbach Corp., *Dimethyl Sulfoxide—Reaction Medium and Reactant,* 1964.

33. Jackson, G.W. and J.S. Dereska, "An electrode mechanism for the electrochemical reduction of m-dinitrobenzene," *J. Electrochem. Soc., 112,* 1218-1221 (1965).

34. Mairanovskii, S.G., "Effect of the double layer structure and of the absorption of electrode reaction participants upon polarographic waves in the reduction of organic substances," *J. Electroanal. Chem., 4,* 166-181 (1962).

35. Given, P.H., M.E. Peover, and J. Schoen, "Polarography of some aromatic carbonyl compounds in dimethylformamide," *J. Chem. Soc., London,* 1958, 2674-2679.

36. Given, P.H., "Polarography of conjugated systems in dimethylformamide," *J. Chem. Soc., London,* 1958, 2684-2687.

37. Hoijtink, G.J., "The polarographic reduction of conjugated hydrocarbons. V. The mechanism of the reduction of various alternant and nonalternant hydrocarbons with aromatic and olefinic double bonds," *Rec. Trav. Chim., 73,* 895-909 (1954).

38. Holleck, L. and D. Becher, "Untersuchungen uber den Einfluss der Leitsalzionen auf die polarographische Reduktion aromatischer Nitroverbindungen in Acetonitril und Dimethylformamid," *J. Electroanal. Chem., 4,* 321 (1962).

APPENDIX I

PURIFICATION OF DMSO

The DMSO used in the solubility experiments had to be purified before use. The DMSO received from Van Waters and Rogers Corp. was in a 46 lb. polyethylene coated container. The principal impurities present were water, dimethyl sulfide and dimethyl sulfone.

Douglas[24] used fractional crystallization to purify his DMSO. Dunnett and Gasser[25] purified the solvent by drying with calcium oxide followed by fractional distillation at 20 mm Hg in a 1 meter column. Meek, Straub, and Drago[26] used a similar method. Sears, Lester, and Dawson[27] also employed fractional distillation at 5 mm Hg. Melendres[5] pretreated the DMSO with sodium hydroxide and molecular sieves before distilling at 5 mm Hg.

The fractional distillation method was used to purify the DMSO used in these studies. The column built for the purpose was modeled after that of Schlaeffer and Schaffernicht.[28] They used vacuum distillation because it was found that DMSO decomposed slightly when distilled at one atmosphere pressure.

The essential features of the distillation apparatus are shown in Figure 21. The column was 1200 mm long with a 25 mm inside diameter. It was well insulated by asbestos cord and spun glass, and was packed with 6 mm Raschig rings. The boiling pot was a 2 liter flask, equipped with a heating mantle. At the top of the column was a water jacketed glass condenser equipped with a teflon stopcock to control the reflux ratio. The collection apparatus consisted of a graduated dispenser of 100 ml capacity and a collection flask which could be withdrawn from the system while the column remained under vacuum. The pressure was measured with a mercury manometer and was maintained by a mechanical vacuum pump isolated from the system by an acetone-dry ice cold trap. The entire apparatus was sealed from the atmosphere and was equipped for dry nitrogen purging.

About 1500 ml of the DMSO as received was placed in the boiling flask and distilled at 3 mm Hg at about 44°C. The first 200 ml of product collected

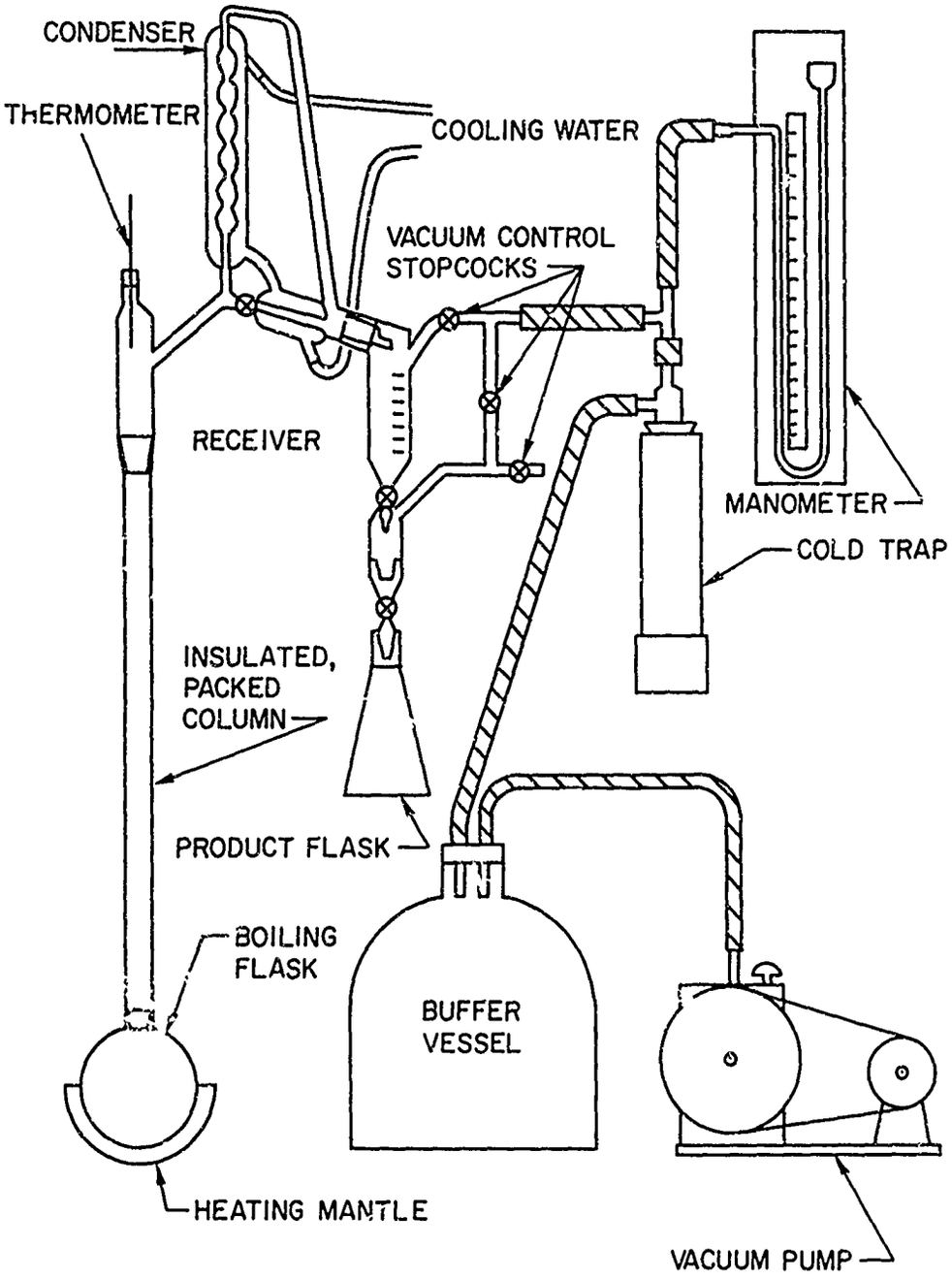

DISTILLATION COLUMN APPARATUS

Figure 21

were discarded. The next 1000 ml of liquid collected were transferred to a flask in a glove box containing a dry nitrogen atmosphere. The final 300 ml were extracted from the boiling flask after the column had been cooled down and were discarded.

The water content of the purified solvent was tested by Karl Fischer titration as described in Appendix III. It was found that the pure DMSO contained less than 100 ppm (.10 weight per cent) water. Some of the properties of the distilled DMSO measured in this laboratory by standard methods, are presented in Table 3. They are in good agreement with the literature values reported by Butler.[4]

TABLE 3

MEASURED PROPERTIES OF PURIFIED DMSO AT 25°C

Density	1.0961 gm/cc
Viscosity	2.011 cp
Dielectric Constant	47.2 ± 2%
Specific Conductance	3.48×10^{-7} $ohm^{-1} cm^{-1}$

APPENDIX II

CALIBRATION OF THE SPECTROPHOTOMETER

The absorbance of m-DNB solutions in DMSO was measured with a Beckman model DU spectrophotometer. Five solutions of known concentration of m-DNB were prepared and their absorbances were measured. The solutions ranged in concentration from zero to 88.44 mg/ml of solution. A wavelength of 420 mμ and a slit width of .22 mm were found to give excellent variations in the absorbance. The readings taken are shown in Table 4.

TABLE 4

CALIBRATION READINGS

Point	Concentration	Absorbance
1	0.00	0.000
2	17.97	0.175
3	30.72	0.300
4	47.43	0.450
5	67.97	0.627
6	88.44	0.785

Since there appeared to be little scatter in the data, it was decided to fit the data to a quadratic equation. In this way it was found that the concentration of an unknown could be determined more easily than from visually picking off a graph.

The region of interest was between 20 and 60 mg/ml, so the points near the center of the data were used to fit the following equation:

$$\text{concentration (mg/ml)} = A\,a^2 + B\,a + D \qquad (44)$$

where a is the absorbance reading, and A, B, and D are constants to be determined.

The following values were found to fit the data well:

$$A = 41.86$$
$$B = 79.98$$
$$D = 2.96$$

The solid line in Figure 22 is the plot of equation with these values for A, B, and D. All solubility data was taken as absorbance readings and converted to concentration in the above manner.

PRECEDING PAGE BLANK

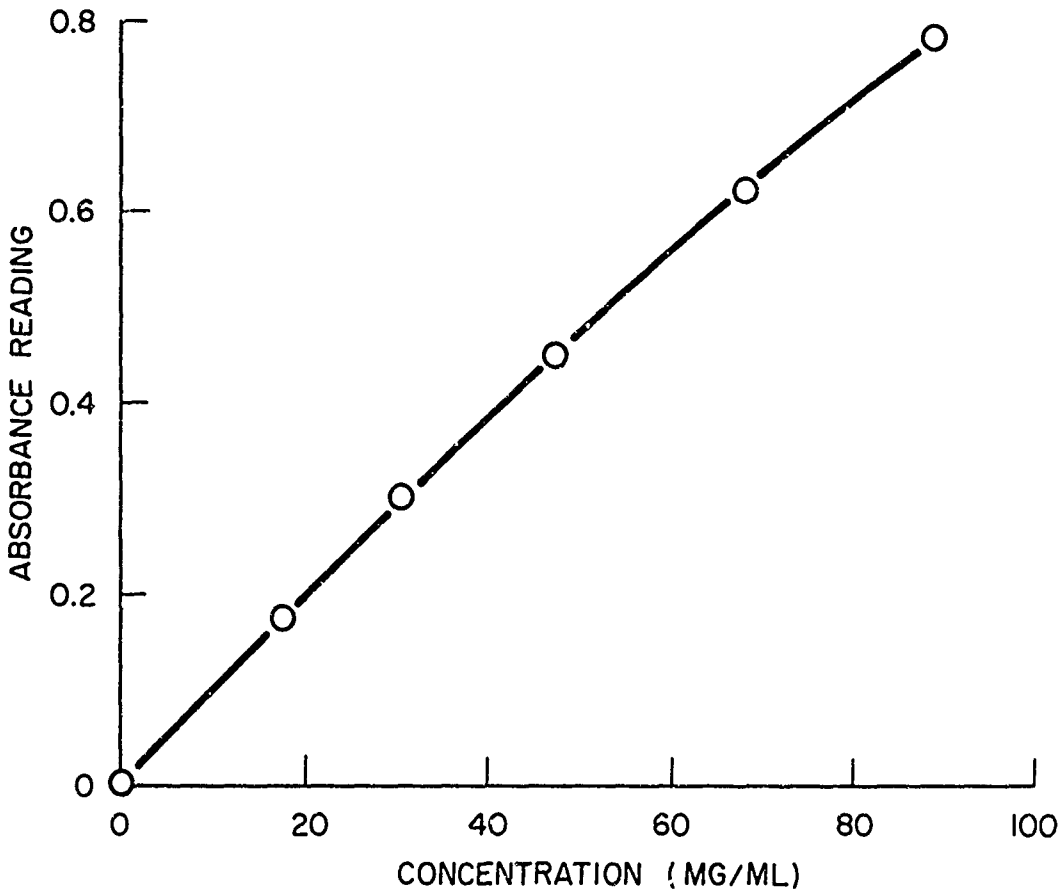

CALIBRATION CURVE FOR DETERMINATION OF m–DNB CONCENTRATION BY SPECTROPHOTOMETRIC MEANS

Figure 22

APPENDIX III

KARL FISCHER WATER DETERMINATION

The hygroscopic nature of DMSO is well known. In addition it has been observed in this laboratory that the addition of water tends to decrease drastically the solubility of m-DNB in DMSO. It was therefore necessary to have some measure of the water content of the purified solvent. This was also necessary to put the purity of the DMSO used into proper perspective when compared to that used by other investigators.

Repeated attempts to determine water content using the Karl Fischer titration method as described by Vogel[29] were unsuccessful. There was difficulty in obtaining a stable end point. Evidently, these difficulties were also encountered by Archer and Jeaters[30] who overcame them by use of a catalyst (ethylpiperidine). The use of the equipment suggested by them improved end point determainations to the extent that reproducible results were obtained.

A standard solution of 1.0 mg/ml water in methanol was used to standardize the stabilized Karl Fischer Reagent (KFR). Both solutions were obtained from Fisher Scientific Co. On different days, the water equivalence of KFR was found to vary randomly between about 1.5 and 2.0 mg H_2O/ml KFR but remained constant for a given determination.

The procedure used was to titrate a solution of absolute methanol and a few drops of 1, 1 ethylpiperidine to the end point with standardized KFR in a sealed cell with a dry nitrogen atmosphere. Then DMSO was introduced into the titration vessel in amounts from 30 to 37 ml. The results are shown in the following table:

TABLE 5

KARL FISCHER WATER DETERMINATION
FOR PURIFIED DMSO

Volume DMSO ml	Volume KFR ml	Equivalence mg H_2O/ml KFR	Water Content ppm
37.05	1.38	1.975	66.8
30.05	0.50	1.975	29.9
34.45	0.57	1.975	29.8
34.5	0.78	1.600	32.9

These samples were taken from the DMSO stored in the dry box for over two weeks after having been distilled one time. On the basis of these results, it is assumed that the water content of the DMSO used in the solubility experiments was below 100 ppm.

APPENDIX IV

MEASUREMENT OF VISCOSITY

The kinematic viscosity of m-DNB solutions in 0.1 M TEAP-DMSO was measured as a function of concentration. A Cannon Ubbelhode Semi-Micro viscometer was used. It was calibrated to have a constant of 0.003910 centistokes/sec. Measurements were done in a constant temperature oil viscometer bath at 24.2°C. Three drop times were recorded at each concentration of m-DNB. The following table gives the results:

Conc. m-DNB	ν (centistokes)
0.00	1.958, 1.954, 1.961
0.01 M	1.989, 1.982, 1.985
0.02 M	2.008, 2.012, 2.018
0.04 M	2.037, 2.045, 2.037

The data is plotted in Figure 23. The values of ν for zero concentration agree very well with those compiled for pure DMSO by Butler.[4]

The purpose of the kinematic viscosity measurements was to get a value which could be used in the expression for the limiting current in rotating disk experiments. Since the kinematic viscosity appears to the 1/6 power, in that expression, the dependence is very insensitive. Therefore an average value of $\nu = .513\ (cm^2/sec)^{1/6}$ was used for all solutions of m-DNB in DMSO for these calculations.

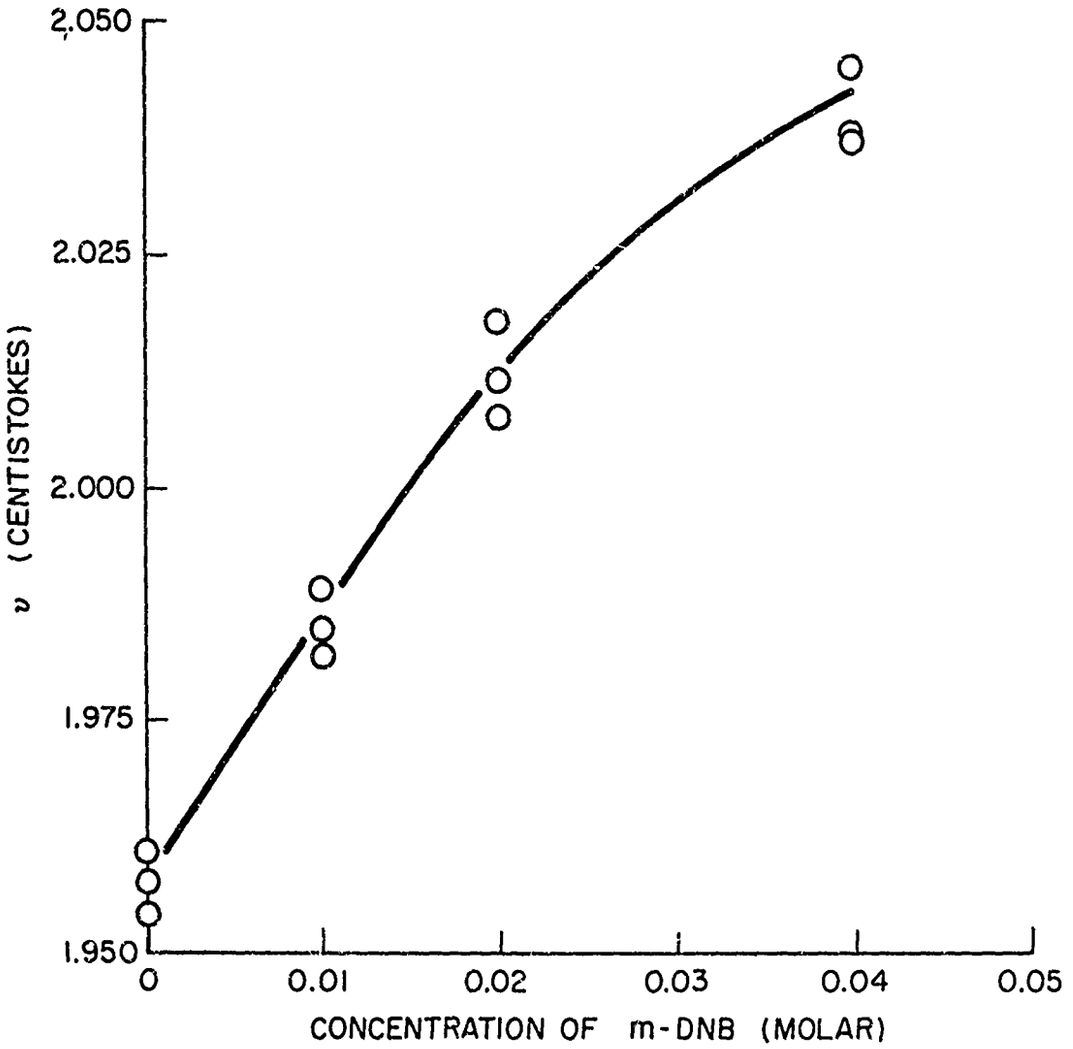

KINEMATIC VISCOSITY OF DMSO SOLUTIONS AS A FUNCTION OF m–DNB CONCENTRATION

Figure 23

APPENDIX V

TEMPERATURE DEPENDENCE OF DIFFUSION COEFFICIENT

A determination of the heights of the first and second waves as a function of temperature was done. It was found that the ratio of the wave heights in the absence of a proton donor was invariant with temperature, as shown by Figure 24. It was hoped that the temperature measurements would held clarify the kinetic steps involved in the second electron transfer. However, the results did not allow additional conclusions to be drawn on this matter.

The temperature measurements were valuable in that they made possible the calculation of the diffusion coefficient of m-DNB as a function of temperature, assuming a 1 electron transfer for the first step. The results are shown in Figure 25. A plot of ln D versus 1/T gives a straight line, as indicated by Figure 26. The slope of this line indicates that the activation energy for diffusion of m-DNB in DMSO is about 3.42 Kcal/mole.

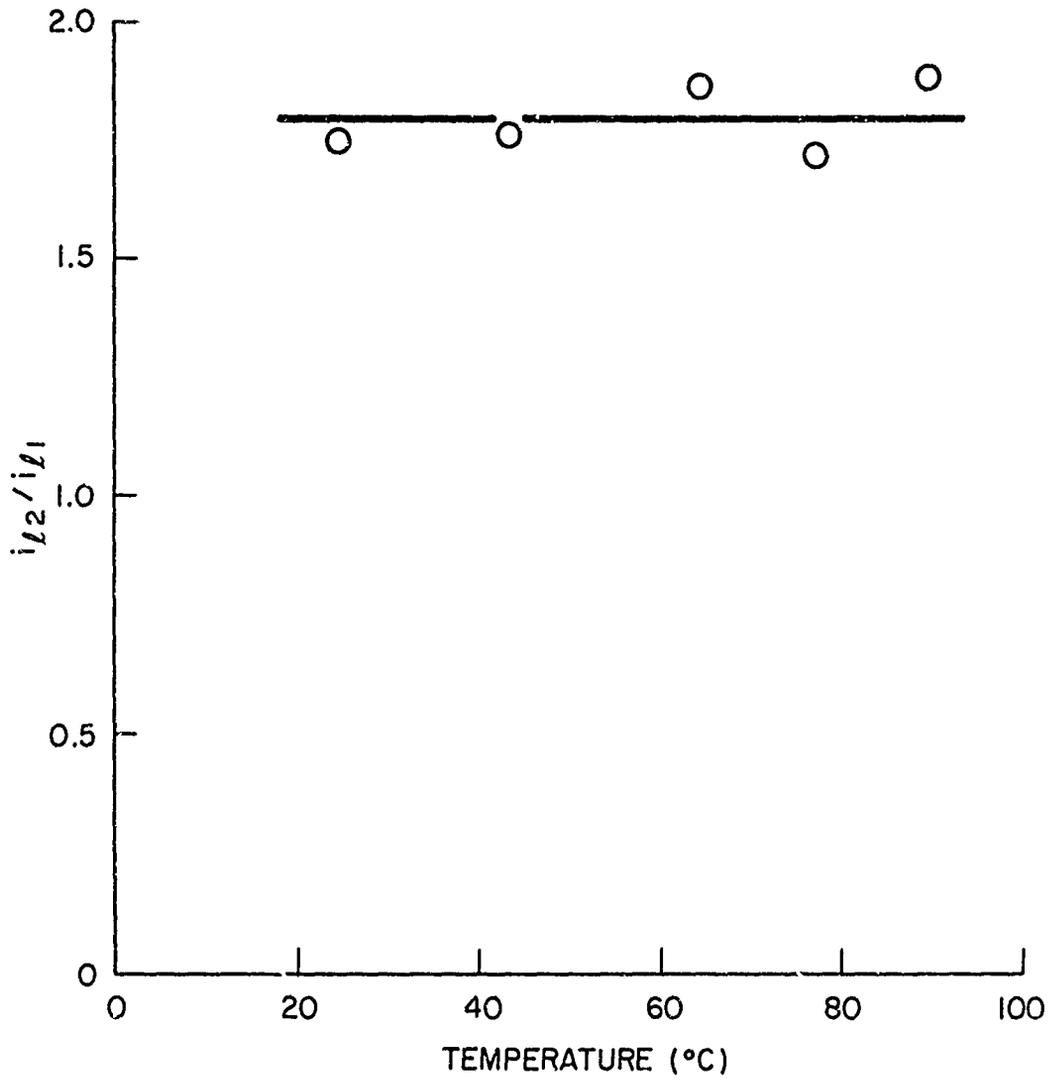

RATIO OF LIMITING CURRENTS FOR 1st AND 2nd WAVES AS A FUNCTION OF TEMPERATURE IN THE ABSENCE OF PROTON DONORS

Figure 24

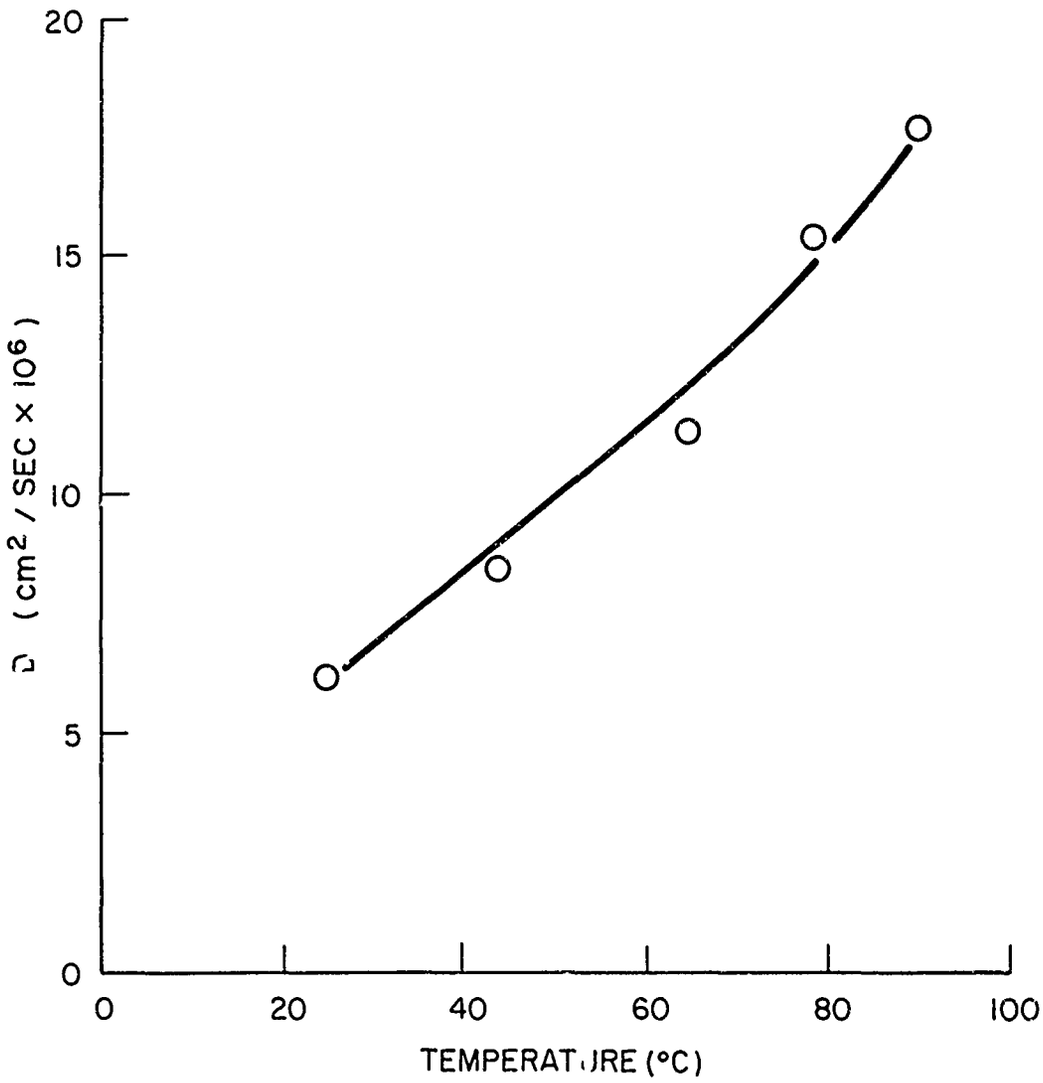

DIFFUSION COEFFICIENT OF m–DNB IN DMSO SOLUTION AS A FUNCTION OF TEMPERATURE

Figure 25

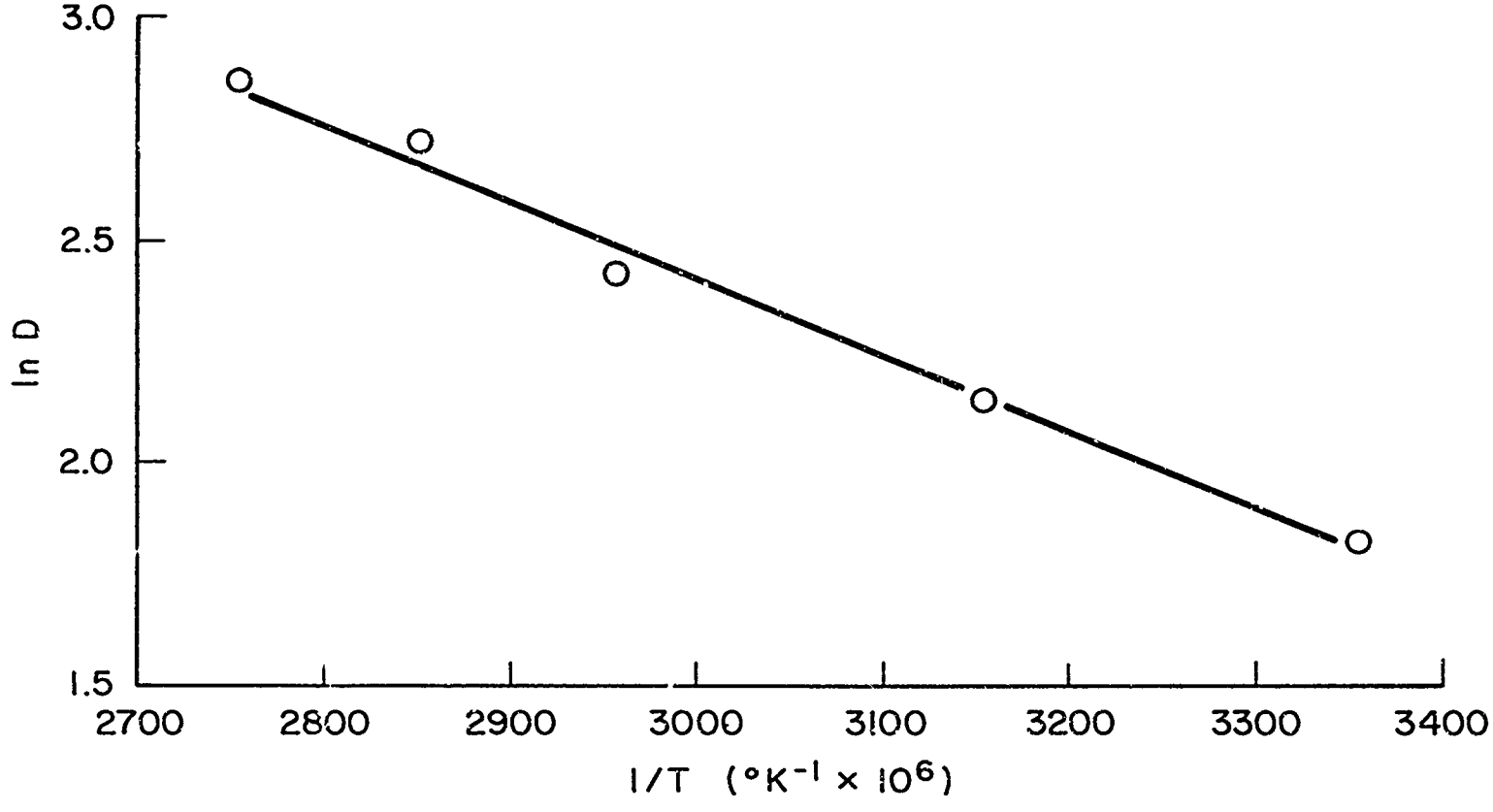

ACTIVATION ENERGY PLOT FOR DIFFUSION OF m–DNB IN DMSO SOLUTION

Figure 26